NACA

RESEARCH MEMORANDUM

THE EFFECTS OF MACH NUMBER AND REYNOLDS NUMBER ON THE AERODYNAMIC CHARACTERISTICS OF SEVERAL 12-PERCENT-THICK WINGS HAVING 35° OF SWEEPBACK AND VARIOUS AMOUNTS OF CAMBER

By Bruce E. Tinling and W. Richard Kolk

Ames Aeronautical Laboratory
Moffett Field, Calif.

NATIONAL ADVISORY COMMITTEE FOR AERONAUTICS

WASHINGTON
February 23, 1951

NATIONAL ADVISORY COMMITTEE FOR AERONAUTICS

RESEARCH MEMORANDUM

THE EFFECTS OF MACH NUMBER AND REYNOLDS NUMBER ON THE AERODYNAMIC CHARACTERISTICS OF SEVERAL 12-PERCENT-THICK WINGS HAVING 35° OF SWEEPBACK AND VARIOUS AMOUNTS OF CAMBER

By Bruce E. Tinling and W. Richard Kolk

SUMMARY

A comparison of the lift, drag, and pitching-moment characteristics of several wings having 35° of sweepback and various amounts of camber has been made from the results of wind-tunnel tests. Six semispan model wings were tested; three having an aspect ratio of 10, and three having an aspect ratio of 5. The streamwise sections for the three wings of each aspect ratio were the NACA 65$_1$A012, the NACA 64$_1$A312, and the NACA 64$_1$A612. The Reynolds number was varied from 2,000,000 to 10,000,000 at a Mach number of 0.25, and the Mach number was varied from 0.25 to 0.92 at a Reynolds number of 2,000,000.

The effects of Reynolds number on the low-speed aerodynamic characteristics were large and were believed to be associated with a reduction of lift on the outer portions of the wing as the Reynolds number was reduced. At low lift coefficients, the effects of increasing the Mach number, up to the Mach number for drag divergence, were to increase the lift-curve slopes of all six wings and to increase the static longitudinal stability of the wings having an aspect ratio of 10. The static longitudinal stability of the wings having an aspect ratio of 5 remained nearly constant within the same range of Mach numbers. As the Mach number for drag divergence was exceeded, the lift-curve slope decreased and a large reduction in static longitudinal stability occurred.

The effects of camber on the maximum lift coefficient, the angle of attack for zero lift, and the pitching-moment coefficient for zero lift were as would be anticipated from the section aerodynamic characteristics. Low-speed results at a Reynolds number of 10,000,000 indicated that camber increased the lift-drag ratio of the wings having an

aspect ratio of 10, but no similar increase was noted for the wings having an aspect ratio of 5.

At high subsonic speeds and a Reynolds number of 2,000,000, camber, in general, reduced the Mach number for drag divergence. At Mach numbers less than that for drag divergence, camber caused considerable improvement in the lift–drag ratio and the pitching–moment characteristics. On the basis of the effects of Reynolds number indicated by the low–speed data, there is doubt that these improvements due to camber would be entirely realized at Reynolds numbers greater than 2,000,000.

INTRODUCTION

The effectiveness of wing sweep in delaying the detrimental effects of compressibility to higher Mach numbers is well known. One of the principal difficulties encountered in the use of swept–back wings of high aspect ratio is the low lift coefficient at which large changes of static longitudinal stability occur. Since this effect is attributed to stalling of the outer portions of the wing, it follows that increase in the lift coefficient at which large changes of static longitudinal stability occur might be realized by increasing the maximum lift coefficient of the wing sections. The use of camber is a familiar means of increasing the maximum lift coefficient as well as the lift–drag ratio of unswept wings. Research on the effects of camber and twist on the aerodynamic characteristics of swept–back wings has been reported in references 1 and 2. The present investigation was initiated to evaluate the effects of camber alone and also the effects of dynamic scale and compressibility on the aerodynamic characteristics of several wings having 35° of sweepback.

Six semispan model wings were tested: Three representing wings having an aspect ratio of 10, and three representing wings having an aspect ratio of 5. The streamwise sections of the three wings of each aspect ratio were the NACA 65_1A012, the NACA 64_1A312, and the NACA 64_1A612. According to simple sweep theory, the aerodynamic characteristics of sections perpendicular to the quarter–chord line determine the aerodynamic characteristics of a swept–back wing. The sections perpendicular to the quarter–chord line of the wings investigated were approximately 14 percent thick and had design lift coefficients of about 0, 0.37, and 0.73. Results of tests of airfoil sections reported in reference 3 have indicated that the addition of camber increases the maximum lift coefficient for airfoil sections having thickness–chord ratios of less than 12 percent, but that the effectiveness of camber in increasing the maximum lift coefficient diminishes as the thickness is increased beyond 12 or 15 percent. For the 14–percent–thick wings tested in the present

investigation, the increase in the maximum lift coefficient resulting from camber and hence the increase in the lift coefficient at which longitudinal instability occurs should be significant but may not be expected to be as great as that which would be anticipated for thinner wings.

The tests were conducted over a range of Mach numbers from 0.25 to 0.92 at a Reynolds number of 2,000,000 and over a range of Reynolds numbers from 2,000,000 to 10,000,000 at a Mach number of 0.25.

NOTATION

C_D drag coefficient $\left(\frac{\text{drag}}{qS}\right)$

$C_{D_{o_{min}}}$ minimum profile-drag coefficient assuming elliptical span load distribution, minimum value of $C_D - \frac{C_L^2}{\pi A}$

C_L lift coefficient $\left(\frac{\text{lift}}{qS}\right)$

C_m pitching-moment coefficient about axis passing through the quarter point of the mean aerodynamic chord $\left(\frac{\text{pitching moment}}{qS\,\bar{c}}\right)$

C_{m_o} pitching-moment coefficient at zero lift

A aspect ratio $\left(\frac{b^2}{2S}\right)$

M Mach number $\left(\frac{V}{a}\right)$

R Reynolds number $\left(\frac{\rho V \bar{c}}{\mu}\right)$

S semispan wing area, square feet

V airspeed, feet per second

L/D lift-drag ratio $\left(\frac{\text{lift}}{\text{drag}}\right)$

[redacted]

a speed of sound, feet per second

b span of complete wing measured perpendicular to the plane of symmetry, feet

c chord, measured parallel to the plane of symmetry, feet

$\bar{c}$ mean aerodynamic chord $\left(\dfrac{\int_0^{b/2} c^2 \, dy}{\int_0^{b/2} c \, dy} \right)$, feet

q dynamic pressure, pounds per square foot

y lateral distance from plane of symmetry, feet

α angle of attack, degrees

α_0 angle of attack for zero lift, degrees

ρ density of air, slugs per cubic foot

μ absolute viscosity, slugs per foot second

MODELS

The six semispan models tested in this investigation were furnished by the Lockheed Aircraft Corporation. Three of the models represented wings having an aspect ratio of 10 and a taper ratio of 0.5; and the other three represented wings having an aspect ratio of 5 and a taper ratio of approximately 0.7. Each model had 35° of sweepback of the quarter-chord line. The dimensions of the models are shown in figure 1.

The thickness distribution of the sections of each model was the same from root to tip and there was no twist. The wing sections in planes parallel to the plane of symmetry were the NACA 65_1A012, the NACA 64_1A312, and the NACA 64_1A612. The wings with these sections will be referred to in this report as the uncambered, moderately cambered, and highly cambered wings, respectively. The mean line of the cambered airfoil sections was the NACA a=0.8 (modified). (See reference 4.) According to simple sweep theory, the aerodynamic characteristics of the wing sections perpendicular to the quarter-chord line determine the aerodynamic characteristics of a swept-back wing. The sections perpendicular to the quarter-chord line of the model wings were about 14 percent thick

and had design lift coefficients of about 0, 0.37, and 0.73 for the uncambered, moderately cambered, and highly cambered wings, respectively. The coordinates of the streamwise sections are tabulated in table I.

The tip of each wing was formed by a half body having a radius equal to the corresponding half thickness of the wing section.

The models were constructed of steel. The outer portions of the model wings having an aspect ratio of 10 were removed and replaced with tip fairings to form the wings having an aspect ratio of 5.

The horizontal turntable upon which the models were mounted in the wind tunnel is directly connected to the balance system. The models were mounted with the root chord in the plane of the turntable as shown in figure 2. The juncture between the models and the turntable was sealed.

TESTS

Two series of tests were conducted: one to evaluate the effects of Reynolds number at a low Mach number, and one to evaluate the effects of compressibility at a constant Reynolds number. The tests to evaluate the effects of Reynolds number were conducted at Reynolds numbers from 2,000,000 to 10,000,000 at a Mach number of 0.25. The tests to evaluate the effects of compressibility were conducted at Mach numbers from 0.25 to 0.92 at a Reynolds number of 2,000,000. Lift, drag, and pitching moment were measured over a range of angle of attack sufficient to obtain lift coefficients from less than zero to that for the stall, except where the range was limited by wind-tunnel power or by the capacity of the force balance.

The dynamic pressure of the tests varied from approximately 90 to 360 pounds per square foot between the Mach numbers of 0.25 and 0.92 at a Reynolds number of 2,000,000, and from approximately 90 to 500 pounds per square foot between the Reynolds numbers of 2,000,000 and 10,000,000 at a Mach number of 0.25. Because of this variation of dynamic pressure, a test was conducted to evaluate the effects of distortion of the model wings under load. This was accomplished by obtaining data at a Reynolds number of 6,000,000 at dynamic pressures of 160 and 310 pounds per square foot which correspond, under the test conditions, to Mach numbers of 0.14 and 0.25, respectively.

[redacted]

CORRECTIONS TO DATA

The data have been corrected for the effects of tunnel-wall interference, including constriction due to the tunnel walls, and approximately for model-support tare forces.

Corrections to the data for the effects of tunnel-wall interference originating from lift on the model have been evaluated by the method of reference 5 using the theoretical span loading for incompressible flow calculated by the method of reference 6. The corrections added to the drag and to the angle of attack were:

For model wings having an aspect ratio of 10:

$$\Delta\alpha = 0.295\ C_L$$

$$\Delta C_D = 0.00472\ C_L^2$$

For model wings having an aspect ratio of 5:

$$\Delta\alpha = 0.263\ C_L$$

$$\Delta C_D = 0.00417\ C_L^2$$

Constriction effects due to the presence of the tunnel walls were computed by the method of reference 7. These corrections have not been modified to allow for the effect of sweep. The magnitude of the corrections to the Mach number and to the dynamic pressure is shown in the following table:

Corrected Mach number	Uncorrected Mach Number		$\frac{q \text{ corrected}}{q \text{ uncorrected}}$	
	A=10	A=5	A=10	A=5
0.700	0.699	0.700	1.002	1.001
.750	.749	.749	1.002	1.001
.800	.798	.799	1.003	1.002
.825	.823	.824	1.003	1.002
.850	.848	.849	1.003	1.002
.875	.872	.873	1.004	1.003
.900	.895	.897	1.005	1.004
.920	.913	.915	1.007	1.005

A correction to the drag data was made to allow for forces on the exposed surface of the turntable. This correction was determined from tests with the model removed from the turntable. The following corrections were subtracted from the measured drag coefficients:

$R \times 10^{-6}$	M	$C_{D_{Tare}}$	
		A=10	A=5
10	0.25	0.0044	0.0066
6	.25	.0045	.0067
4	.25	.0046	.0069
2	.25	.0050	.0076
2	.40	.0053	.0080
2	.60	.0056	.0085
2	.70	.0058	.0089
2	.75	.0060	.0091
2	.80	.0062	.0094
2	.825	.0063	.0096
2	.85	.0064	.0097
2	.875	.0066	.0100
2	.90	.0067	.0102
2	.92	.0068	.0103

No attempt was made to evaluate tares due to interference between the model and the turntable or to compensate for the tunnel-floor boundary layer which, at the turntable, had a displacement thickness of one-half inch.

RESULTS AND DISCUSSION

Model Distortion Under Aerodynamic Loads

The results of the tests to determine the effect of changes of the dynamic pressure on the aerodynamic characteristics due to bending and twisting of the uncambered model wing having an aspect ratio of 10 are presented in figure 3. Any sizable difference in the amount of bending and twisting of the model wing occurring between dynamic pressures of 160 and 310 pounds per square foot would cause a difference in the slopes of the lift and of the pitching-moment curves. Since the slopes of the curves presented in figure 3 are very nearly the same for both dynamic pressures, except near the maximum lift coefficient, it may be concluded that the effects of model distortion were negligible. The increase of maximum lift coefficient at a Mach number of 0.14 (q,160)

[redacted]

over that at a Mach number of 0.25 (q,310) is consistent with the effects of Mach number on the maximum lift coefficient reported in reference 8.

Effects of Reynolds Number

The results of tests conducted to evaluate the effects of Reynolds number at a Mach number of 0.25 are presented in figure 4. These results show that the aerodynamic characteristics in the upper lift-coefficient range were sensitive to changes in the Reynolds number. In this upper lift-coefficient range a large reduction of static longitudinal stability occurred. This reduction, which may be correlated with a decrease in lift-curve slope, is believed to have been caused by a decrease of the lift-curve slopes of the outer sections of the wings. Increasing the Reynolds number mitigated this reduction in static longitudinal stability and increased the lift-curve slopes of the wings at the higher lift coefficients. Increasing the Reynolds number also caused a large increase in the maximum lift coefficient for all six wings.

An increase in the Reynolds number resulted in a slightly less negative angle of attack for zero lift for the cambered wings. In general, the effects of Reynolds number on the pitching-moment coefficient near the design lift coefficient of each wing (approximately equal to the streamwise section design lift coefficient multiplied by the cosine of 35°) were small. The change in the pitching-moment coefficient for zero lift with increasing Reynolds number for the uncambered wing which had an aspect ratio of 10 (fig. 4(a)) is not clearly understood. This change, however, in the pitching-moment coefficient for zero lift is believed to have been caused by a difference between the effects of Reynolds number on the chordwise extent of the laminar boundary layer on the upper and lower surfaces of the wing.

Lift-drag ratios computed from the data of figure 4 are presented in figure 5. An increase of the Reynolds number from 2,000,000 to 10,000,000 increased the lift-drag ratio at high lift coefficients for all six wings and decreased the maximum lift-drag ratio of all but the aspect-ratio-10 highly cambered wing.

A discontinuity occurred in the lift, drag, and pitching-moment data for the uncambered wings at a lift coefficient of approximately 0.2 at a Reynolds number of 2,000,000. (See figs. 4(a) and 4(d).) This discontinuity is associated with termination of the low-drag range of the airfoil sections rather than any three-dimensional effect. The variations of profile-drag coefficient (assuming elliptical span load distribution) and the pitching-moment coefficient are presented as functions of lift coefficient in figure 6. From these data it may be seen that

the discontinuity in the pitching-moment data occurred at the same lift coefficient as the increase in drag corresponding to the termination of the low-drag range. Increasing the Reynolds number from 2,000,000 to 10,000,000 reduced the positive lift coefficient at which the low-drag range was terminated from approximately 0.2 to 0.1.

Effects of Mach Number

The data obtained from tests at a Reynolds number of 2,000,000 for a range of Mach numbers from 0.25 to 0.92 are presented in figures 7 through 12. The lift coefficient at which an abrupt decrease in static longitudinal stability occurred, which can be correlated with a decrease in the lift-curve slope, increased with increasing Mach number up to the Mach number where there occurred nearly simultaneously a decrease of lift-curve slope, a decrease of stability, and a drag rise. This Mach number will be referred to in this report as the force-divergence Mach number.

The data in figure 13 show the effect of Mach number on the pitching-moment-curve slope $\partial C_m/\partial C_L$, the lift-curve slope $\partial C_L/\partial \alpha$, and the drag coefficients for the six wings at lift coefficients near their respective design values. These data show that the lift-curve slope of each wing increased with Mach number up to the force-divergence Mach number. For this same Mach number range, the wings which had an aspect ratio of 5 were approximately neutrally stable about the quarter point of the mean aerodynamic chord. The slopes of the pitching-moment curves $\partial C_m/\partial C_L$ of the wings which had an aspect ratio of 10 were approximately -0.06 at a Mach number of 0.25 and, in general, became more negative, indicating increasing static longitudinal stability, as the Mach number for force-divergence was approached. For the wings of both aspect ratios, serious static longitudinal instability resulted when the Mach number for force divergence was exceeded.

Effects of Camber

Discussion of the effects of camber is complicated by the differences in the thickness distributions between the cambered and the uncambered wings, the streamwise thickness distribution of the cambered wings being the NACA 64_1A012 and that of the uncambered wings being the NACA 65_1A012. An estimate of the probable difference in the maximum lift coefficient between swept-back wings having NACA 64_1A012 and NACA 65_1A012 sections has been made through the use of simple sweep theory. According to simple sweep theory, the differences in the maximum lift coefficients of the sections perpendicular to the quarter-chord

line must be found in order to evaluate the difference in the maximum lift coefficients of wings having different streamwise sections. The thickness of the airfoil sections perpendicular to the quarter-chord line of the subject wings was approximately 14 percent of the chord. Data presented in reference 3 show that at a Reynolds number of 6,000,000 (equivalent Reynolds number of about 9,000,000 based on the swept wing of this investigation), the section maximum lift coefficient of the uncambered 14-percent thick 64-series airfoil section is approximately 4 percent greater than that for the uncambered 14-percent-thick 65-series airfoil section. This same percentage increase in the maximum lift coefficient may also be expected to exist between the NACA 65A- and 64A-series sections according to results presented in reference 4. The effect of variations in the section-thickness distributions on the data obtained at high Mach numbers is believed to be small in view of the results of the investigation reported in reference 9 which indicate that the lift- and drag-divergence Mach numbers for the 12-percent-thick 65-series and 64-series airfoil sections are nearly the same over a wide range of lift coefficients.

It must be noted that the results of tests of airfoil sections reported in reference 3 have indicated that the addition of camber increases the maximum lift coefficient for airfoil sections having thickness-chord ratios of less than 12 percent, but that the effectiveness of camber in increasing the maximum lift coefficient diminishes as the thickness ratio is increased beyond 12 or 15 percent. Since the sections perpendicular to the quarter-chord line of the wings tested in this investigation were about 14 percent thick the increase due to camber in the maximum lift coefficient and hence the lift coefficient at which a change in static longitudinal stability occurs would not be expected to be as great as that for thinner wings.

The lift, drag, and pitching-moment characteristics of the wings with various amounts of camber are presented in figure 14 for a Mach number of 0.25 and a Reynolds number of 10,000,000. The values of pertinent aerodynamic parameters taken from the data of figure 14 are presented in the following tables:

ASPECT RATIO 10			
Parameter	Airfoil section		
	NACA 65_1A012	NACA 64_1A312	NACA 64_1A612
Design C_L	0	0.25	0.50
$(\partial C_L/\partial\alpha)_{\text{design } C_L}$	.075	.075	.075
$^1C_{L_{max}}$	.97	1.24	1.32
α_o	0	−2.2°	−4.4°
$(\partial C_m/\partial C_L)_{\text{design } C_L}$	−.071	−.046	−.100
C_{m_o}	−.006	−.048	−.090
$C_{D_{o_{min}}}$	.0052	.0060	.0064
$(L/D)_{max}$	32.5	34.0	35.0
C_L for $(L/D)_{max}$	.38	.40	.49

[1]At R, 6,000,000 (fig. 4.)

ASPECT RATIO 5			
Parameter	Airfoil section		
	NACA 65_1A012	NACA 64_1A312	NACA 64_1A612
Design C_L	0	0.25	0.50
$(\partial C_L/\partial\alpha)_{\text{design } C_L}$	.063	.064	.064
$C_{L_{max}}$	1.00	1.32	1.44
α_o	0	−2.2	−4.4
$(\partial C_m/\partial C_L)_{\text{design } C_L}$	.002	.006	−.016
C_{m_o}	.002	−.046	−.091
$C_{D_{o_{min}}}$	.0053	.0066	.0073
$(L/D)_{max}$	22.5	22.5	21.5
C_L for $(L/D)_{max}$	.29	.29	.32

The principal effects of increasing camber, as would be anticipated from airfoil-section aerodynamic characteristics, were an increase in the maximum lift coefficient, a decrease in the angle of attack for zero lift, and an increase in the negative value of the pitching-moment coefficient at zero lift.

[redacted]

Camber improved the maximum lift–drag ratio of the wings which had an aspect ratio of 10, the maximum lift–drag ratio of the highly cambered wing being roughly 10 percent greater than that for the uncambered wing. (See fig. 15.) However, no improvement was observed in the maximum lift–drag ratio of the wings having an aspect ratio of 5. The lift–drag ratio at high values of lift coefficient for the wings of both aspect ratios was improved by camber because of the higher maximum lift coefficient of the cambered wings.

Comparison of the pitching–moment data of figure 14 for the wings having an aspect ratio of 10 indicates that a moderate amount of camber lessened the changes in static longitudinal stability at lift coefficients greater than 0.6. This was the only instance for which the static longitudinal stability was improved in the upper–lift–coefficient range by camber at a Mach number of 0.25 and a Reynolds number of 10,000,000. The instability of the uncambered wings in the upper–lift–coefficient range was not accompanied by a large drag rise and is therefore believed to have been due to trailing–edge separation. Furthermore, measurements of surface static pressures on the uncambered wing of aspect ratio 5 at a Reynolds number of 10,000,000 and a Mach number of 0.25 showed that initial flow separation on this wing was in the region of the trailing edge. From consideration of two–dimensional section characteristics, camber could be expected only to aggravate the trailing–edge separation. This possibly accounts for the lack of any consistent significant improvement due to camber in static longitudinal stability in the upper–lift–coefficient range.

Comparison of the data for the three wings of each aspect ratio obtained at a Reynolds number of 2,000,000 indicates that, at this low Reynolds number, camber caused marked improvement in the aerodynamic characteristics at high lift coefficients. Such a comparison may be made from data presented in figure 16 which were obtained at a Mach number of 0.25. Inspection of these data reveals that, in addition to improving the maximum lift coefficient, camber caused increases in the lift coefficient at which static longitudinal instability occurred and reduced the drag coefficient at large values of lift coefficient.

Comparison of the data of figures 7 through 12, which are for Mach numbers from 0.25 to 0.92 and a Reynolds number of 2,000,000, indicates that the improvements due to camber in the maximum lift coefficient and in the lift coefficient at which static longitudinal instability occurred were maintained at Mach numbers up to the force–divergence Mach number. In addition, the lift data show that the angle of attack for zero lift of the cambered wings became less negative as the Mach number was increased beyond 0.80.

The pitching–moment coefficients for given values of lift coefficient are presented as functions of Mach number in figure 17. These

data show that the pitching-moment coefficients of the cambered wings became more negative with increasing Mach number up to the force-divergence Mach number where an abrupt positive increase in the pitching-moment coefficients occurred.

The drag coefficients of the six wings for several lift coefficients are presented in figure 18 as functions of Mach number. The Mach numbers for drag divergence, specifically defined as the Mach numbers at which $\frac{\partial C_D}{\partial M} = 0.1$ from figure 18, are presented in the following table:

C_L	A = 10			A = 5		
	NACA 65_1A012	NACA 64_1A312	NACA 64_1A612	NACA 65_1A012	NACA 64_1A312	NACA 64_1A612
0	0.89	0.88	---	0.88	0.87	---
.2	.87	.85	0.82	.85	.84	0.82
.4	.84	.82	.80	.82	.79	.78
.6	---	.75	.75	---	.76	.74
.8	---	.73	.71	---	.75	.72

As would be anticipated from the results of tests of 64-series airfoil sections reported in reference 10, the drag-divergence Mach number was, in general, reduced by camber. At Mach numbers less than that for drag divergence, the effect of camber was to reduce the drag for values of lift coefficient greater than 0.2. At a lift coefficient of 0.6, the drag of the uncambered wings was large and erratic due to the proximity of this lift coefficient to the maximum lift coefficient for these wings. For the same reason, the drag of the moderately cambered wings was much greater than that of the highly cambered wings for a lift coefficient of 0.8.

The variation of lift-drag ratio with lift coefficient is shown in figures 19 and 20. At Mach numbers less than 0.80, the maximum lift-drag ratio of the moderately cambered wing which had an aspect ratio of 10 was considerably greater than that of the uncambered wing. The maximum lift-drag ratio of the highly cambered wing which had an aspect ratio of 10, however, was only slightly greater than that for the uncambered wing at Mach numbers less than 0.70. The improvement due to camber in the maximum lift-drag ratio of the wings which had an aspect ratio of 5 was less than that for the wings which had an aspect ratio of 10. In fact, no improvement due to camber for the wings having an aspect ratio of 5 was realized at Mach numbers greater than 0.60.

Camber caused large increases in the lift-drag ratio in the upper-lift-coefficient range. This was true for the wings of both aspect ratios provided the Mach number for drag divergence was not exceeded, a result which would be anticipated from the results of tests of 64-series airfoil sections reported in reference 10.

It is emphasized, however, that the effects of Reynolds number must be considered in any attempt to assess the benefits derived from the use of camber on these wings at the higher Mach numbers. The effects of camber on the static longitudinal stability and on the lift-drag ratio varied with the test Reynolds number. This variation may be seen by comparing figures 14 and 15 (Reynolds number, 10,000,000) with figures 16, 19, and 20 (Reynolds number, 2,000,000). These data show that the improvement in the lift-drag ratio and in the pitching-moment characteristics due to camber were, in general, much smaller at a Reynolds number of 10,000,000. Therefore, there is considerable doubt that the improvements due to camber for lift coefficients less than the maximum of the uncambered wings, indicated to exist at Mach numbers greater than 0.25 at a Reynolds number of 2,000,000, can be entirely realized at full-scale Reynolds numbers.

CONCLUSIONS

Six semispan model wings were tested: three having an aspect ratio of 10, and three having an aspect ratio of 5. The streamwise airfoil sections for the three wings of each aspect ratio were the NACA 65_1A012, the NACA 64_1A312, and the NACA 64_1A612. Results of this investigation indicated the following:

1. The effects on the aerodynamic characteristics of an increase in Reynolds number from 2,000,000 to 10,000,000 at a Mach number of 0.25 were large.

2. For the wings having an aspect ratio of 10, at a Reynolds number of 10,000,000 and a Mach number of 0.25, the maximum lift-drag ratio was improved by camber. No similar improvements were found for the wings having an aspect ratio of 5.

3. The effects of camber on the maximum lift coefficient, the angle of attack for zero lift, the pitching-moment coefficient for zero lift, and the Mach number for drag divergence of these wings were consistent with those which would be anticipated from section aerodynamic characteristics.

[redacted]

4. An abrupt decrease of the lift-curve slope, which was accompanied by a large reduction in static longitudinal stability, occurred nearly simultaneously with drag divergence for all six wings.

5. At Mach numbers less than that for drag divergence and at a Reynolds number of 2,000,000, camber increased the lift-drag ratio and the lift coefficient at which a decrease of static longitudinal stability occurred. If the effects of Reynolds number indicated by the low-speed test results prevail, however, these improvements at the higher Mach numbers would not be entirely realized at Reynolds numbers greater than 2,000,000.

Ames Aeronautical Laboratory,
National Advisory Committee for Aeronautics,
Moffett Field, California.

REFERENCES

1. Jones, J. Lloyd, and Demele, Fred A.: Aerodynamic Study of a Wing-Fuselage Combination Employing a Wing Swept Back 63°. — Characteristics Throughout the Subsonic Speed Range with the Wing Cambered and Twisted for a Uniform Load at a Lift Coefficient of 0.25. NACA RM A9D25, 1949.

2. Hunton, Lynn W.: Effects of Twist and Camber on the Low-Speed Characteristics of a Large-Scale 45° Swept-Back Wing. NACA RM A50A10, 1950.

3. Abbott, Ira H., von Doenhoff, Albert E., and Stivers, Louis S., Jr.: Summary of Airfoil Data. NACA Rep. 824, 1945.

4. Loftin, Laurence K., Jr.: Theoretical and Experimental Data for a Number of NACA 6A-Series Airfoil Sections. NACA Rep. 903, 1948. (Formerly NACA TN 1368.)

5. Sivells, James C., and Deters, Owen J.: Jet-Boundary and Plan-Form Corrections for Partial-Span Models with Reflection Plane, End Plate, or No End Plate in a Closed Circular Wind Tunnel. NACA Rep. 843, 1946.

6. DeYoung, John, and Harper, Charles W.: Theoretical Symmetric Span Loading at Subsonic Speeds for Wings Having Arbitrary Plan Form. NACA Rep. 921, 1948.

7. Herriot, John G.: Blockage Corrections for Three-Dimensional-Flow Closed-Throat Wind Tunnels, with Consideration of the Effect of Compressibility. NACA RM A7B28, 1947.

8. Sprieter, John R., and Steffen, Paul J.: Effect of Mach and Reynolds Numbers on Maximum Lift Coefficient. NACA TN 1044, 1946.

9. Van Dyke, Milton D., and Wibbert, Gordon A.: High-Speed Aerodynamic Characteristics of 12 Thin NACA 6-Series Airfoils. NACA MR A5F27, 1945.

10. Summers, James L., and Treon, Stuart L.: The Effects of Amount and Type of Camber on the Variation with Mach Number of the Aerodynamic Characteristics of a 10-Percent-Thick NACA 64A-Series Airfoil Section. NACA TN 2096, 1950.

[redacted]

TABLE I.- STREAMWISE AIRFOIL COORDINATES

[All dimensions given in percent chord]

(a) NACA 65_1A012

Upper and lower surfaces	
Station	Ordinate
0	0
.5	.913
.75	1.106
1.25	1.414
2.5	1.942
5.0	2.614
7.5	3.176
10	3.647
15	4.392
20	4.956
25	5.383
30	5.693
35	5.897
40	5.995
45	5.977
50	5.828
55	5.544
60	5.143
65	4.654
70	4.091
75	3.467
80	2.798
85	2.106
90	1.413
95	.719
100	.025
L. E. radius: 0.922-percent c	
T. E. radius: 0.029-percent c	

(b) NACA 64_1A312, a=0.8 (modified) mean line

Upper surface		Lower surface	
Station	Ordinate	Station	Ordinate
0	0	0	0
.364	1.036	.636	.867
.598	1.267	.902	1.029
1.078	1.635	1.422	1.273
2.299	2.324	2.701	1.691
4.774	3.320	5.226	2.238
7.265	4.085	7.735	2.626
9.763	4.726	10.237	2.937
14.773	5.745	15.227	3.403
19.793	6.523	20.207	3.732
24.820	7.108	25.180	3.954
29.850	7.530	30.150	4.084
34.883	7.800	35.116	4.128
39.919	7.911	40.081	4.074
44.955	7.834	45.045	3.892
49.990	7.600	50.010	3.610
55.022	7.233	54.978	3.255
60.051	6.753	59.949	2.848
65.076	6.171	64.924	2.406
70.096	5.494	69.904	1.946
75.113	4.736	74.887	1.496
80.135	3.898	79.865	1.094
85.135	2.959	84.868	.795
90.093	1.995	89.907	.524
95.047	1.010	94.953	.274
100	.025	100	.025
L. E. radius: 0.994-percent c			
T. E. radius: 0.028-percent c			

(c) NACA 64_1A612, a=0.8 (modified) mean line

Upper surface		Lower surface	
Station	Ordinate	Station	Ordinate
0	0	0	0
.236	1.093	.764	.755
.454	1.358	1.046	.882
.912	1.786	1.588	1.062
2.103	2.612	2.897	1.346
4.552	3.834	5.448	1.670
7.033	4.790	7.967	1.872
9.529	5.599	10.471	2.021
14.547	6.900	15.453	2.216
19.587	7.906	20.413	2.324
24.640	8.676	25.360	2.368
29.701	9.246	30.299	2.356
34.768	9.632	35.232	2.288
39.838	9.827	40.162	2.155
44.910	9.805	45.090	1.919
49.980	9.596	50.020	1.614
55.044	9.223	54.956	1.265
60.102	8.705	59.898	.895
65.151	8.050	64.849	.522
70.192	7.264	69.808	.168
75.225	6.351	74.775	-.131
80.269	5.290	79.731	-.318
85.262	4.028	84.738	-.300
90.184	2.721	89.816	-.221
95.094	1.373	94.906	-.099
100	.025	100	-.025
L. E. radius: 0.994-percent c			
T. E. radius: 0.028-percent c			

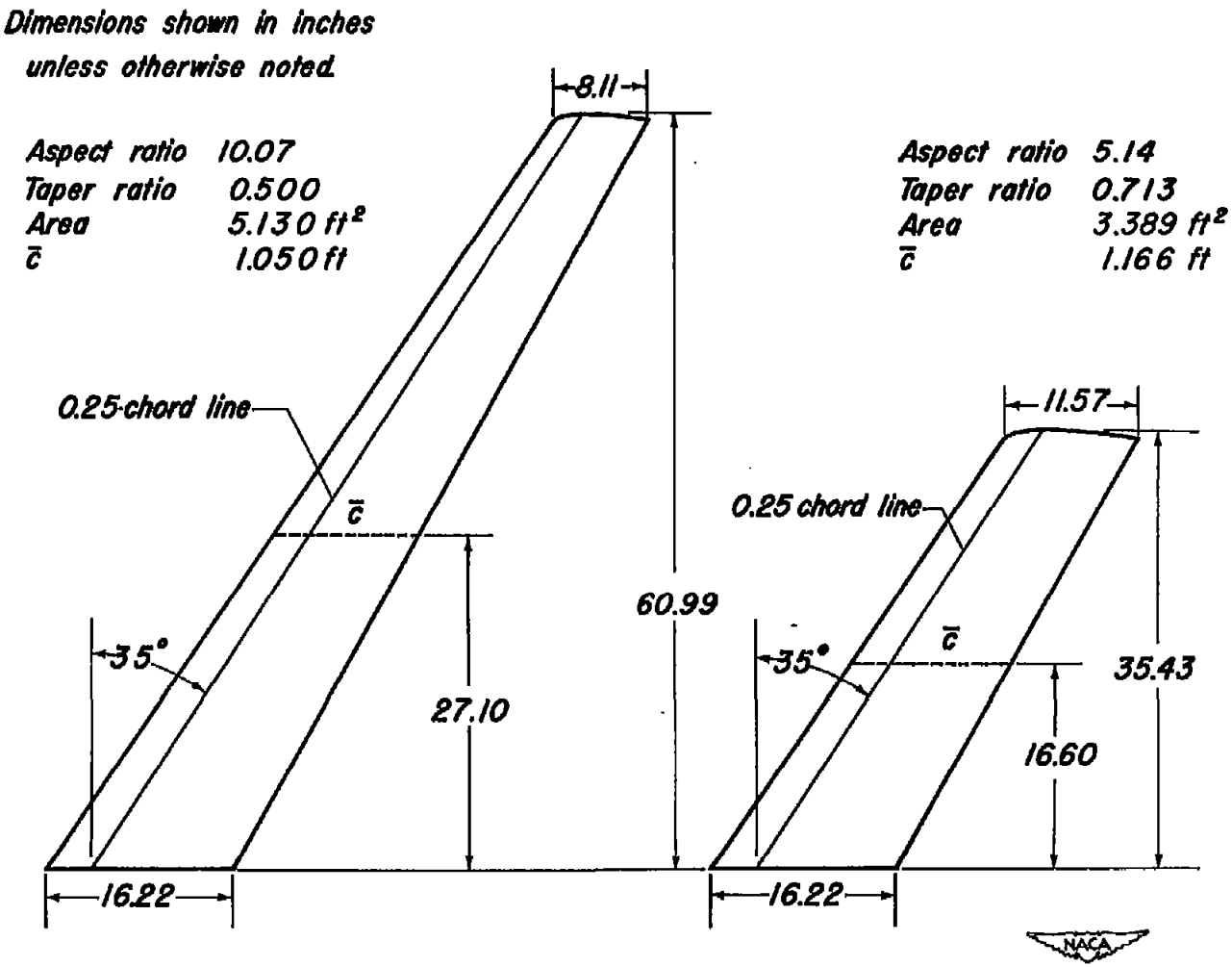

Coordinates of the airfoil sections are tabulated in table I.

Figure 1.– Plan forms of the semispan models.

Figure 2.- Semispan model wing of aspect ratio 10 mounted in the Ames 12-foot pressure wind tunnel.

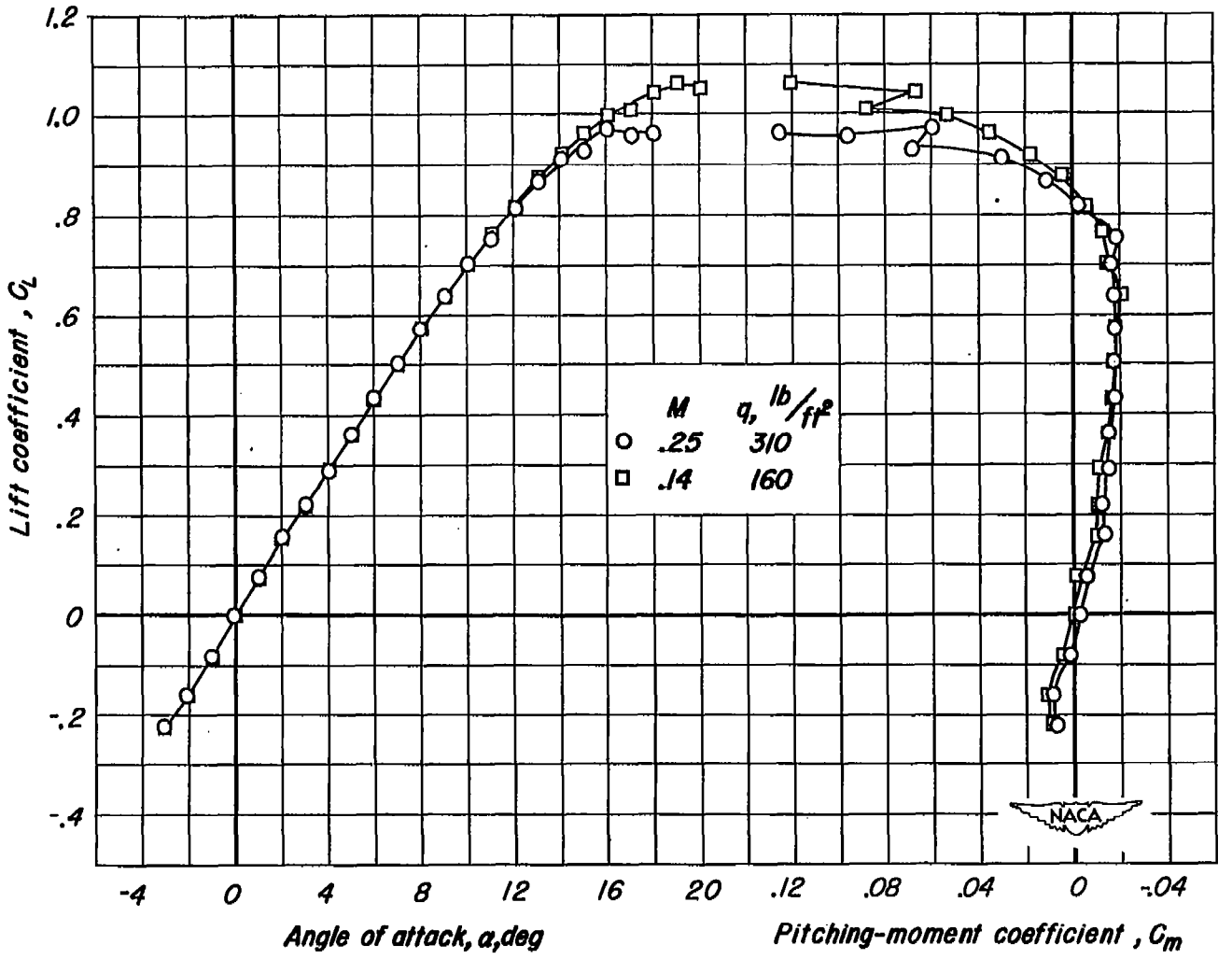

Figure 3.- The lift and pitching-moment characteristics at two dynamic pressures. A, 10; airfoil section, NACA 65,A012; R, 6,000,000.

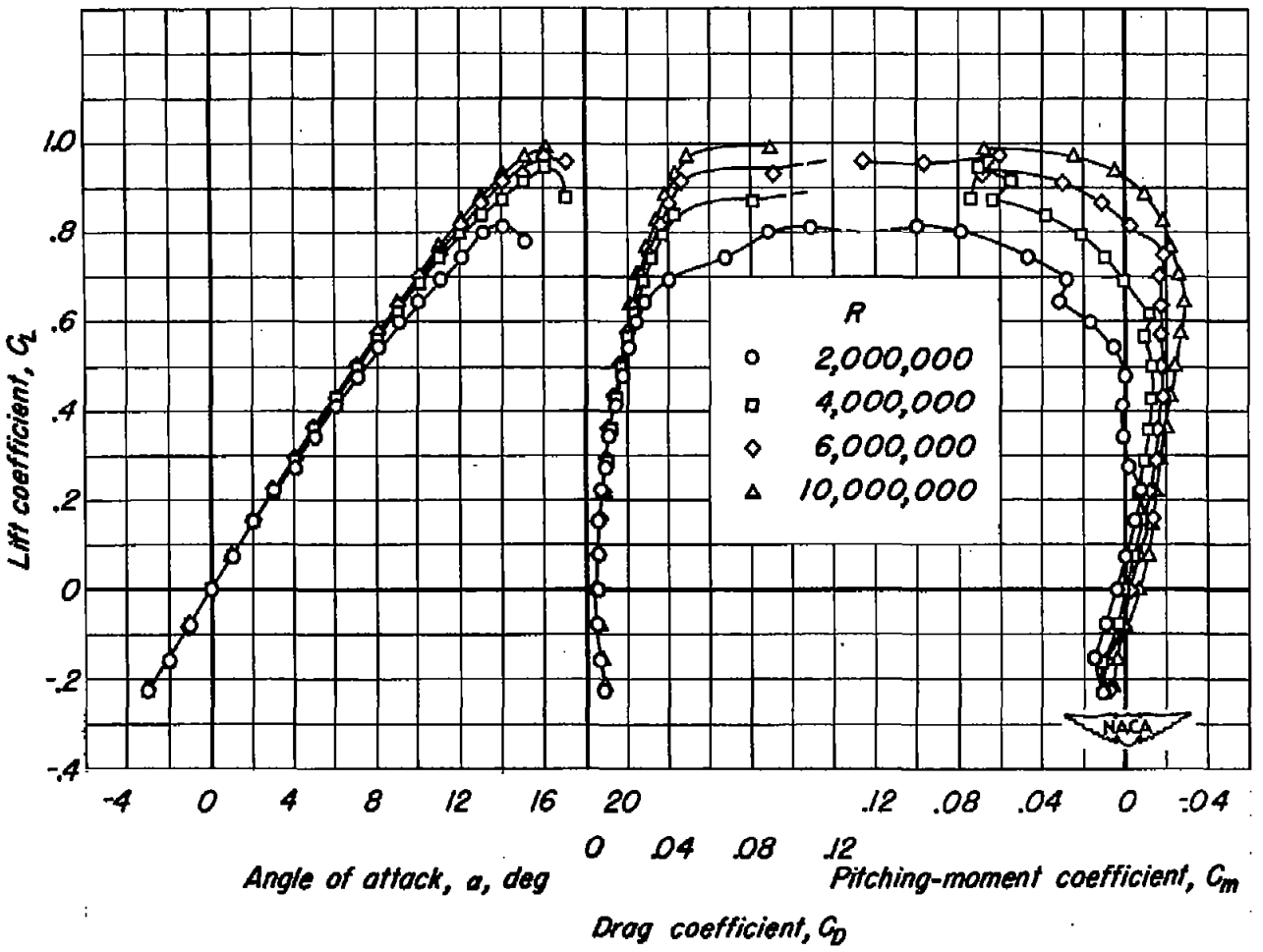

(a) A, 10; airfoil section, NACA 65,A012.

Figure 4.- The effect of Reynolds number on the low-speed aerodynamic characteristics. M,0.25.

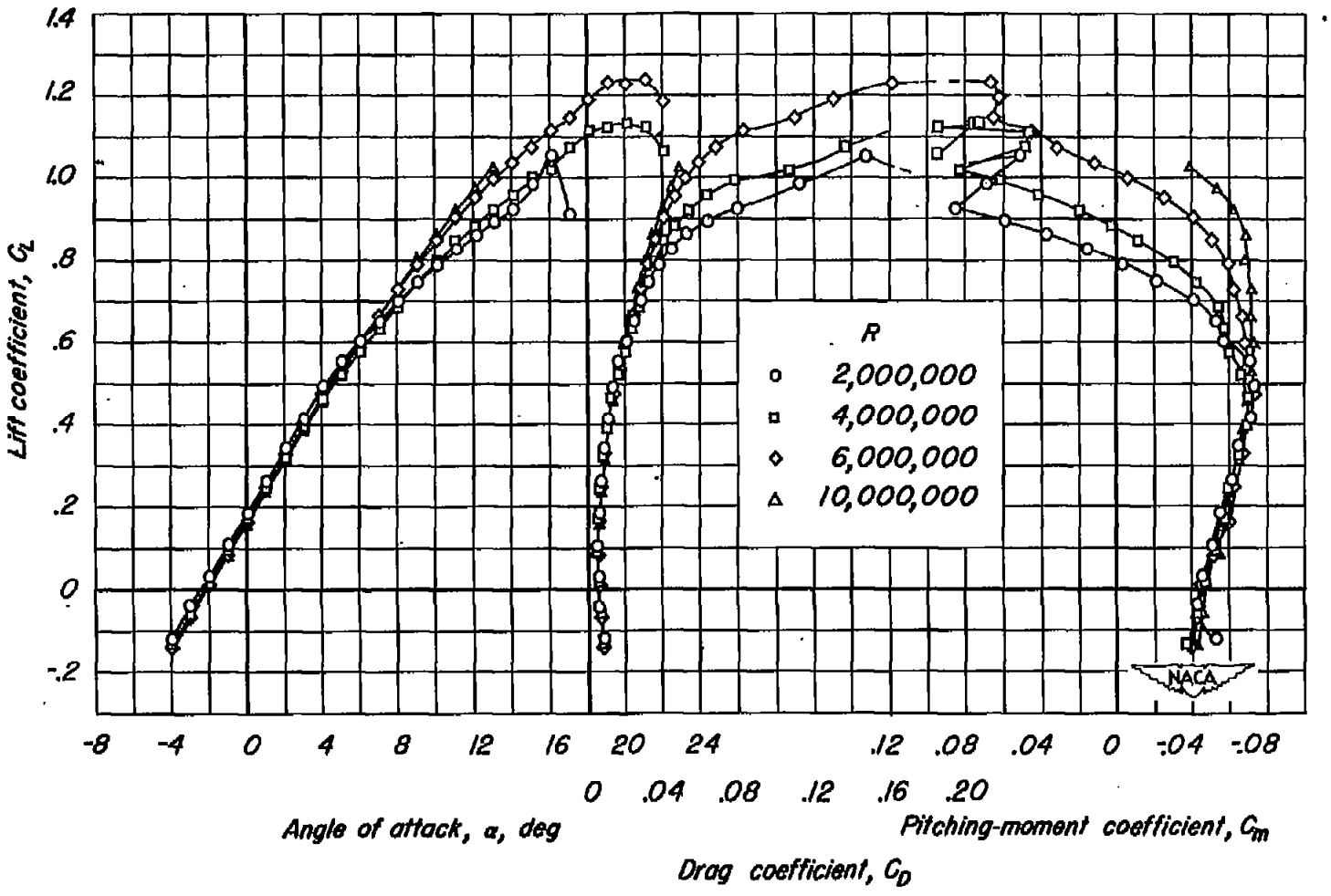

(b) A, 10; airfoil section, NACA 64,A312.

Figure 4.- Continued.

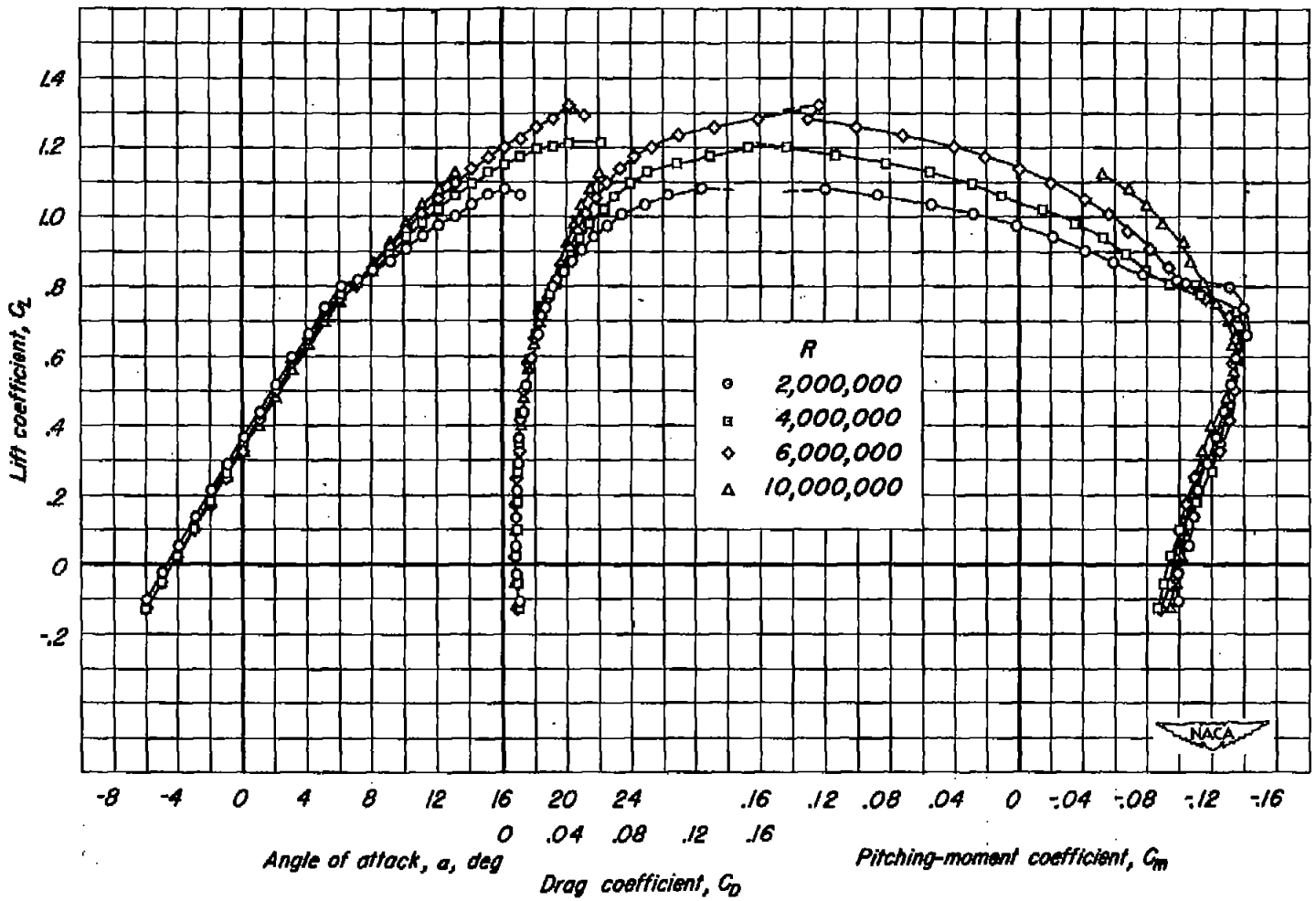

(c) A, 10; airfoil section, NACA 64₁A612.

Figure 4.— Continued.

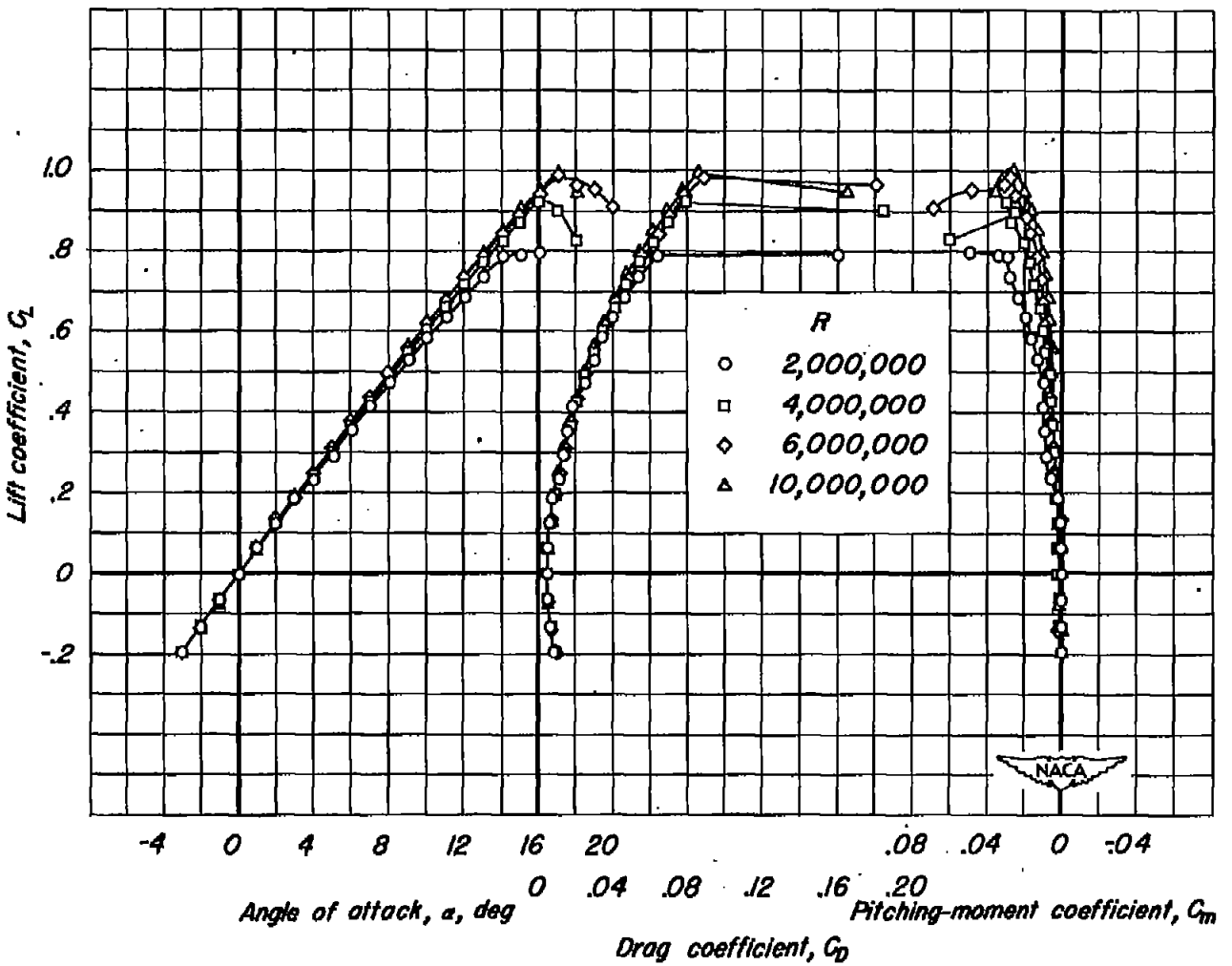

(d) A, 5; airfoil section, 65₁A012.

Figure 4.— Continued.

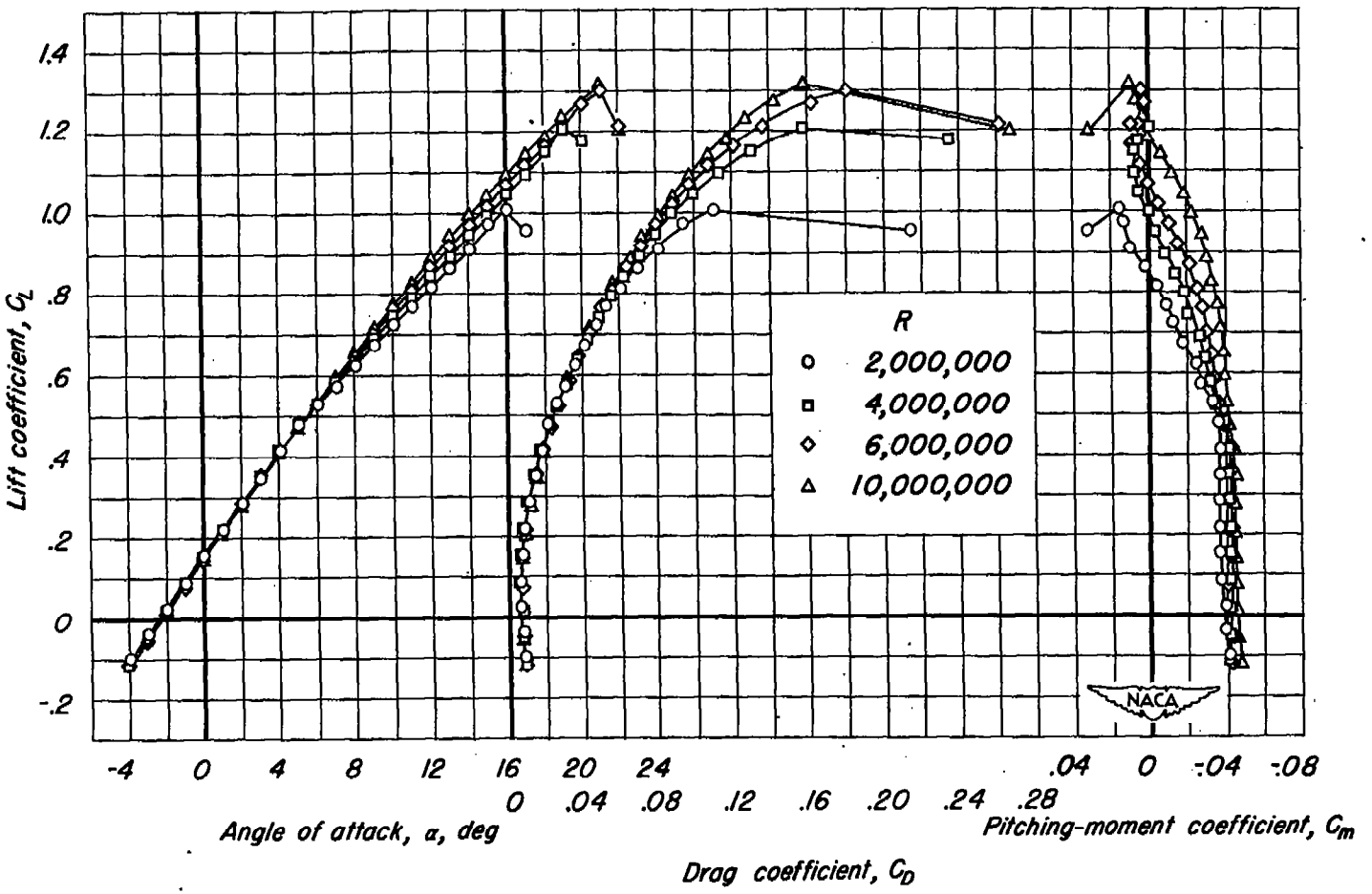

(e) A, 5; airfoil section, NACA 64$_1$A312.

Figure 4.— Continued.

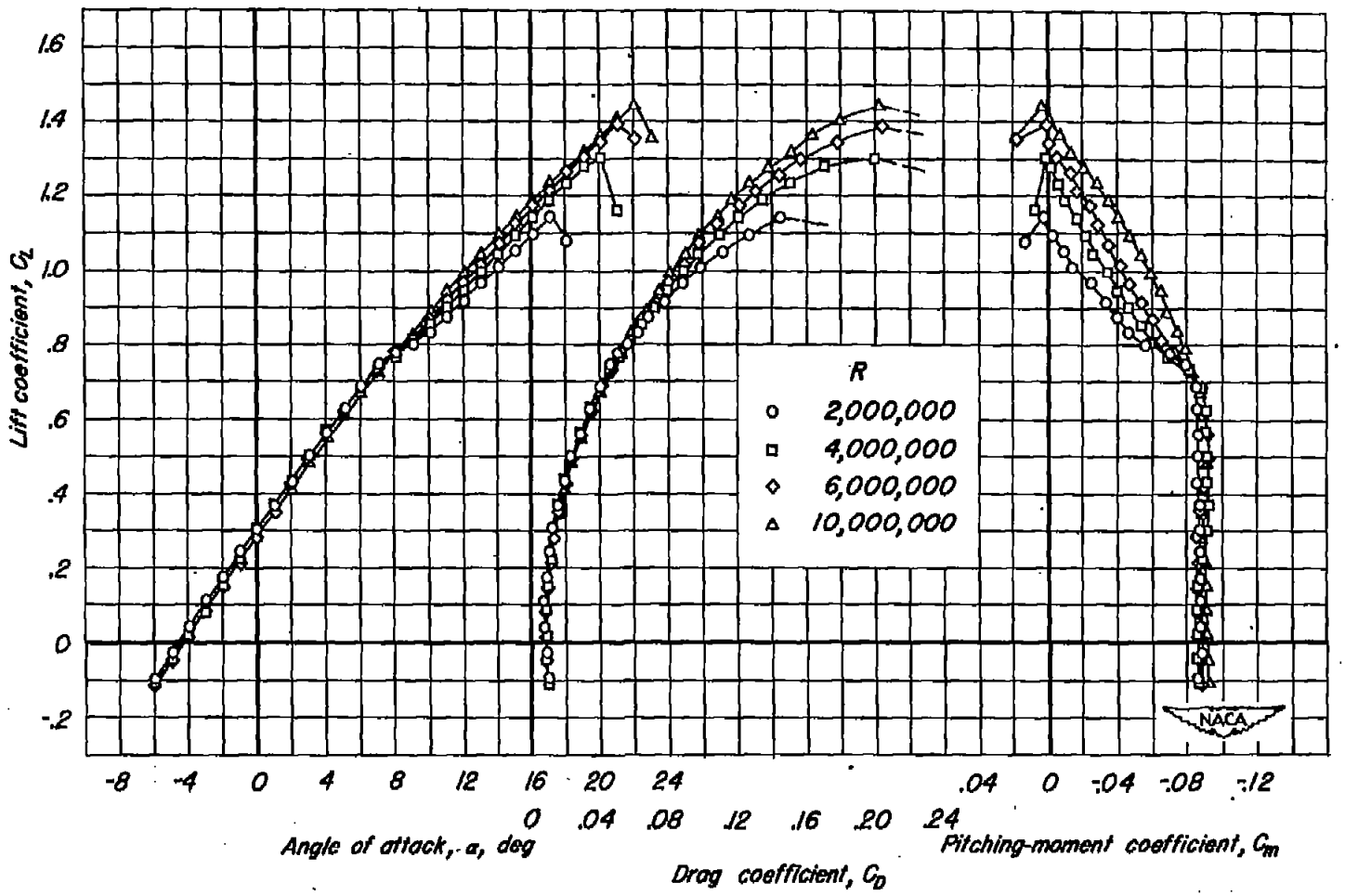

(f) $A_3 5_1$ airfoil section, NACA 64$_1$A612.

Figure 4.- Concluded.

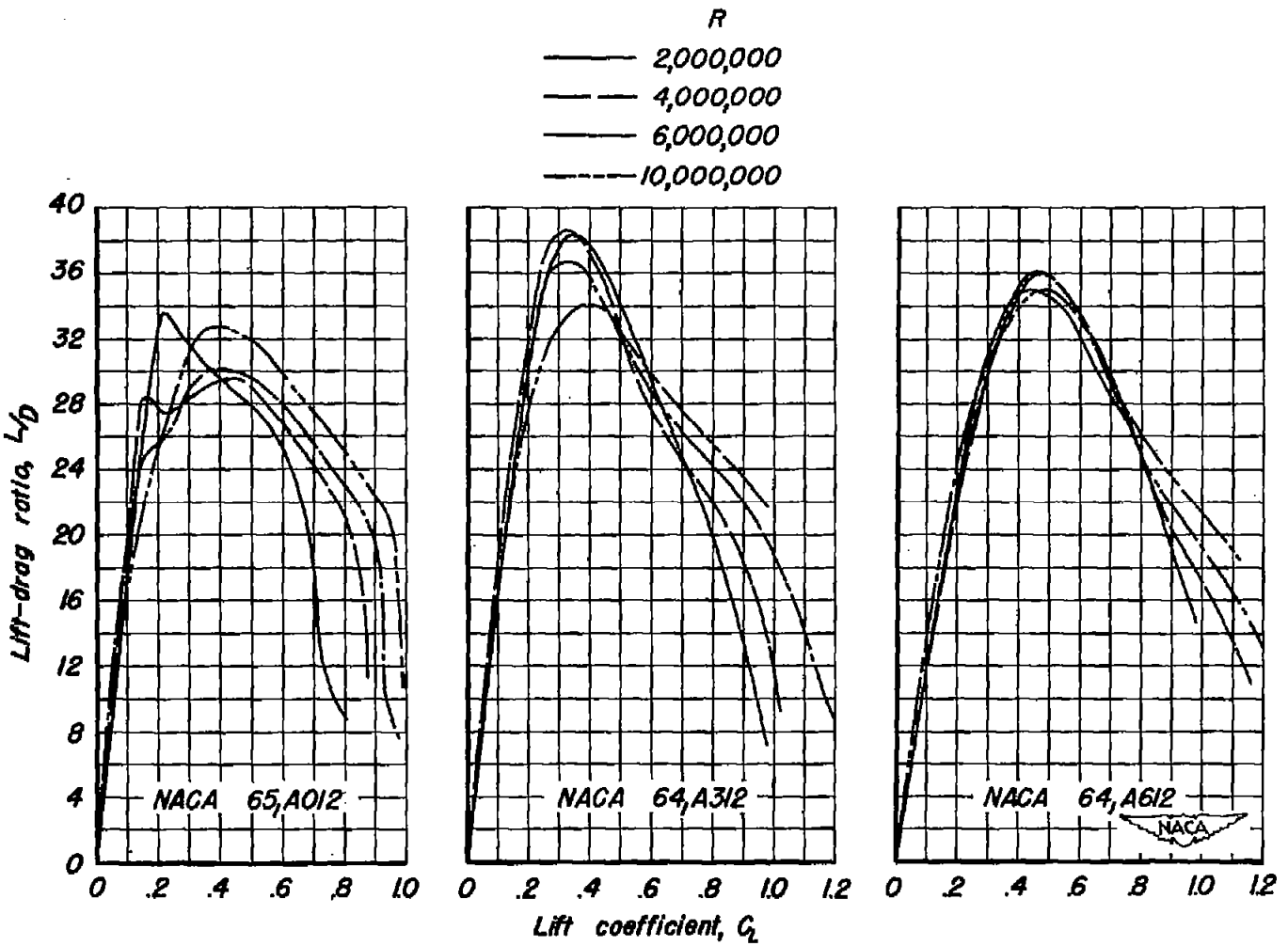

(a) A, 10.

Figure 5.– The effect of Reynolds number on the lift-drag ratio at low speed. M, 0.25.

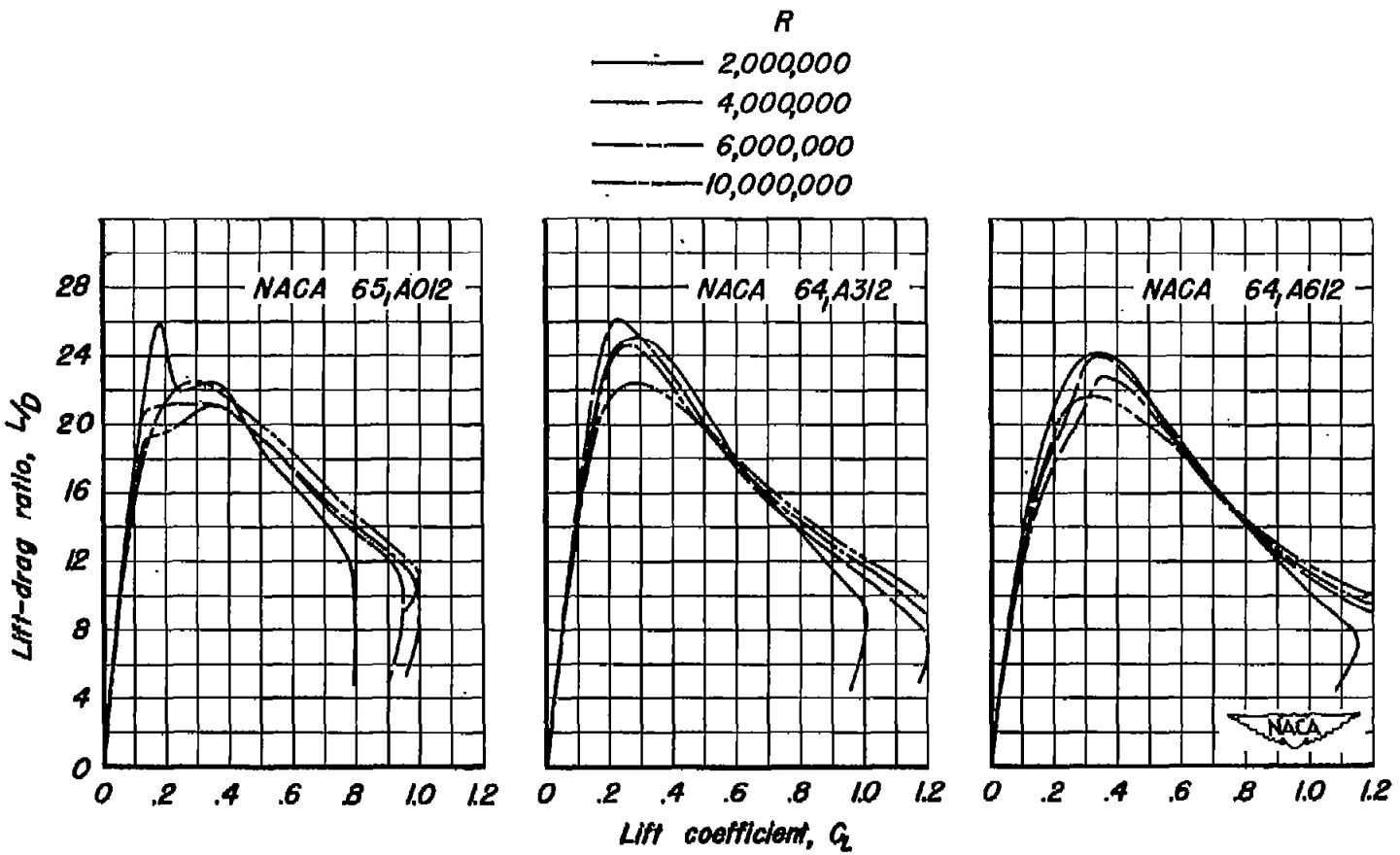

(b) A, 5.

Figure 5.- Concluded.

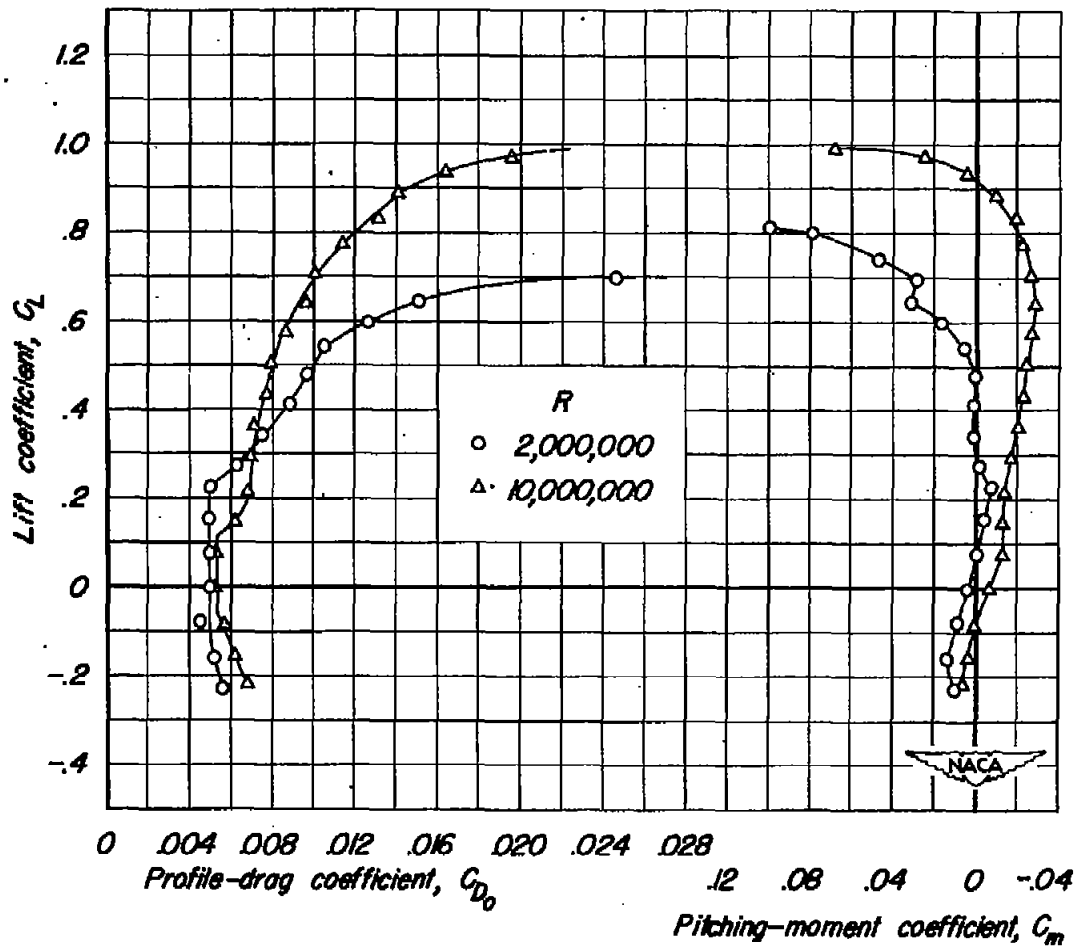

(a) A, 10.

Figure 6.- The variation of profile-drag coefficient and pitching-moment coefficient with lift coefficient. M, 0.25; Airfoil section NACA 65,A012.

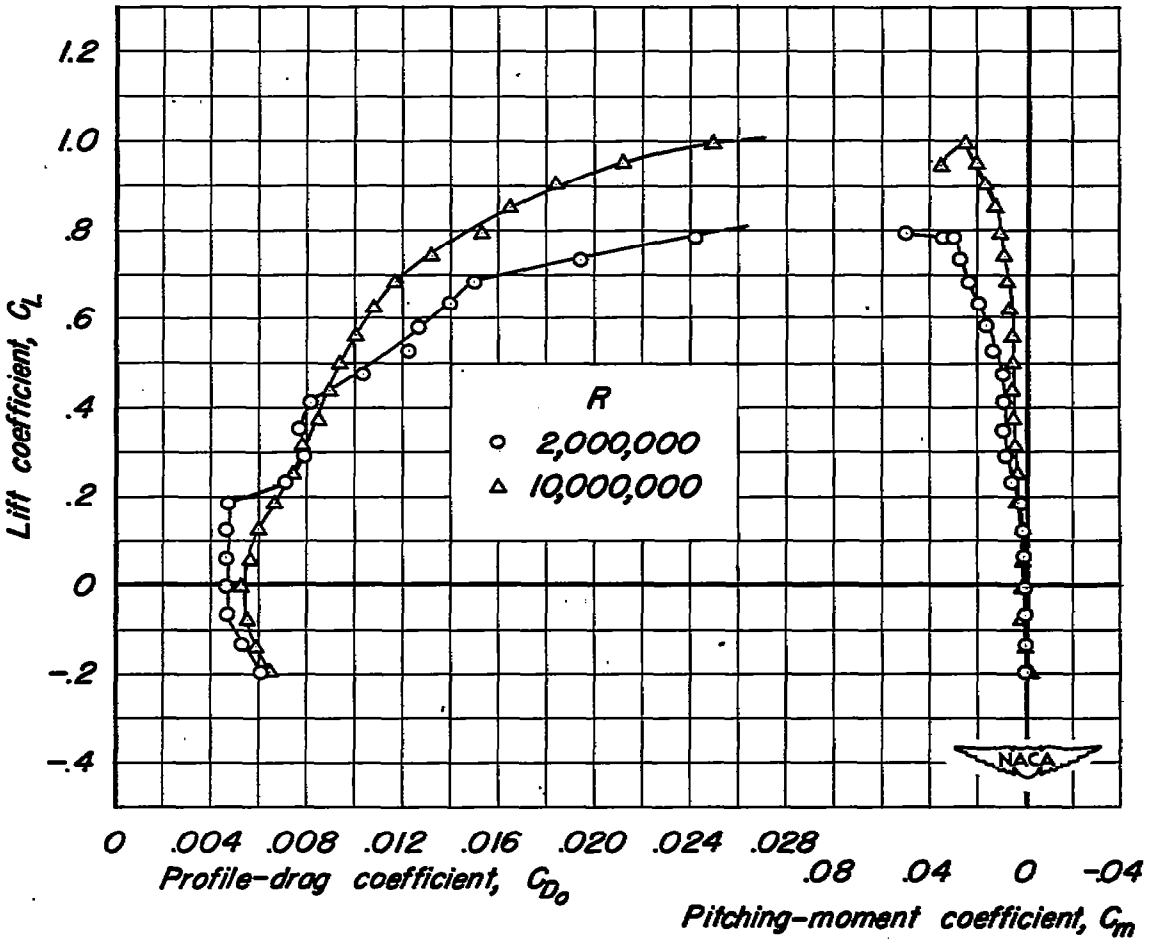

(b) A, 5.

Figure 6.- Concluded.

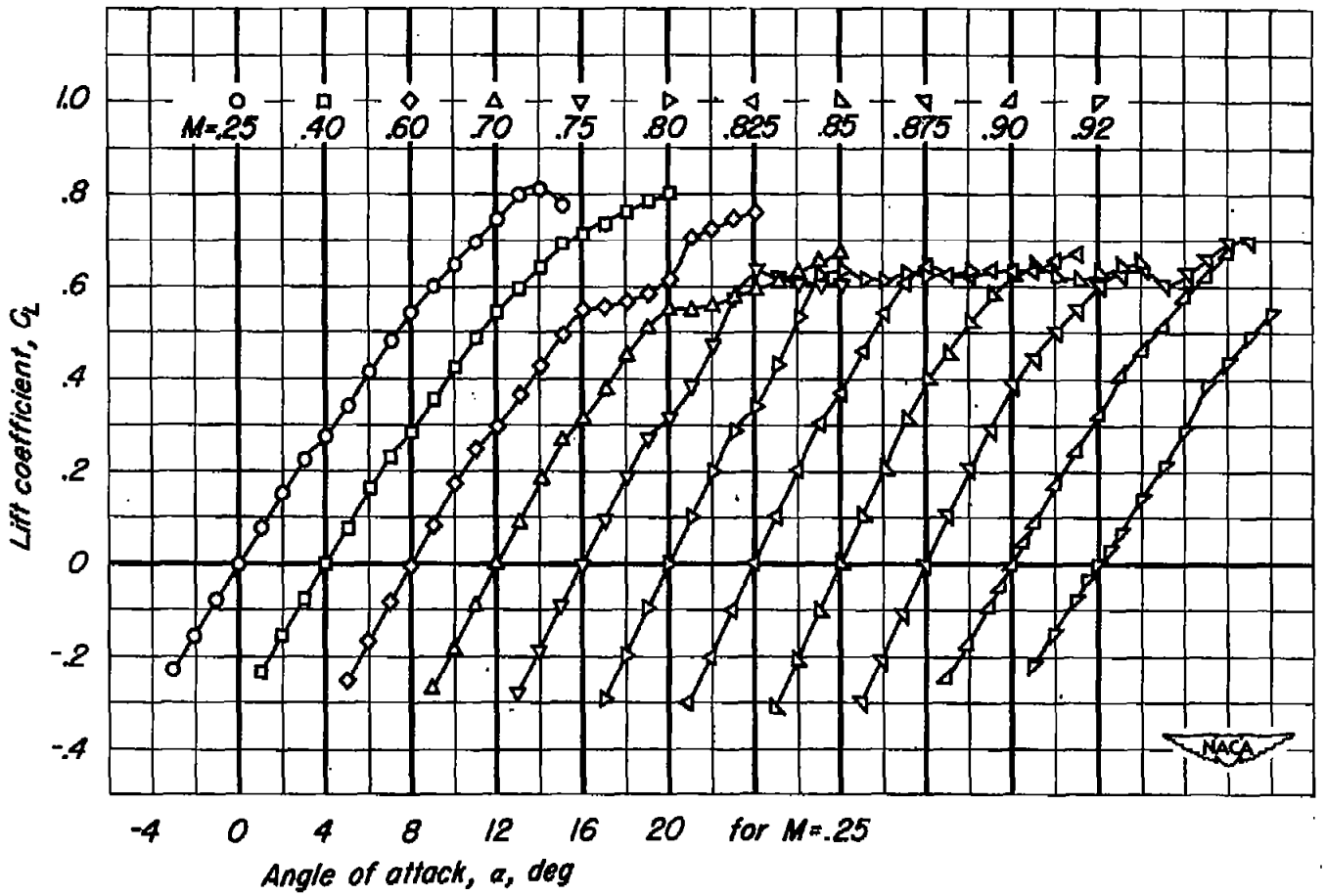

(a) C_L vs α.

Figure 7.— The effect of Mach number on the aerodynamic characteristics. A, 10; airfoil section, NACA 65,A012; R, 2,000,000.

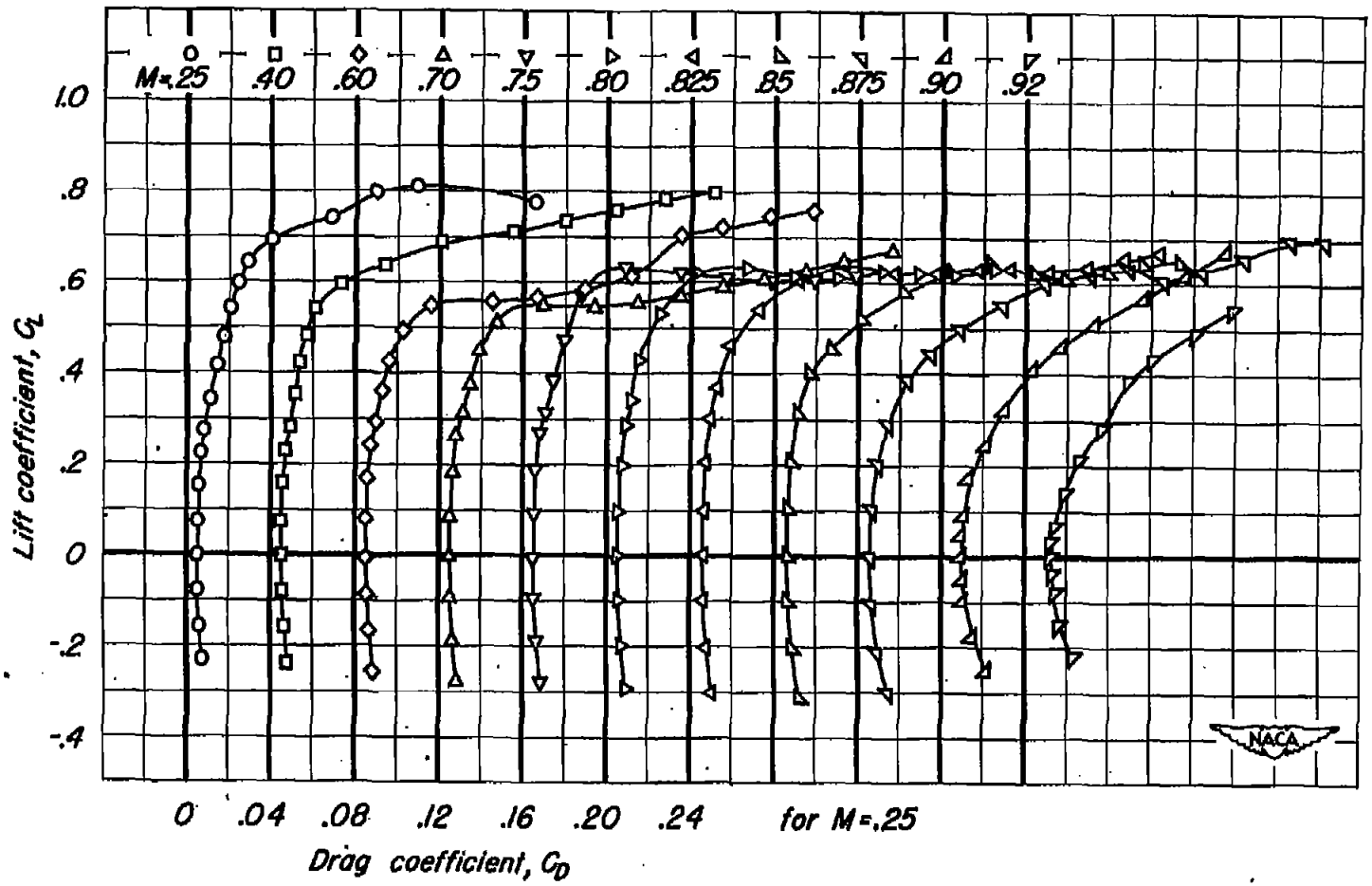

(b) C_L vs C_D.

Figure 7.– Continued.

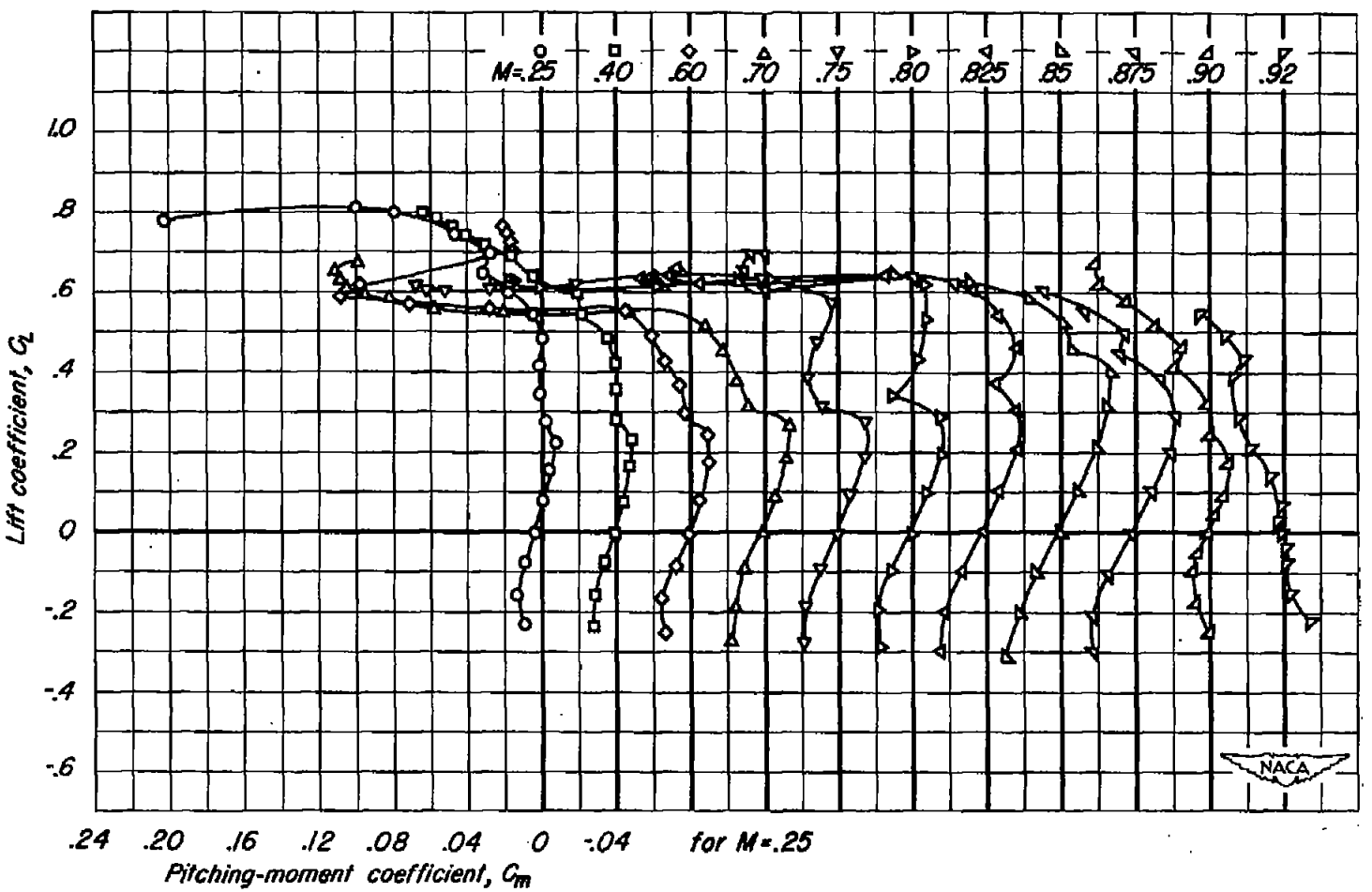

(c) C_L vs C_m.

Figure 7.- Concluded.

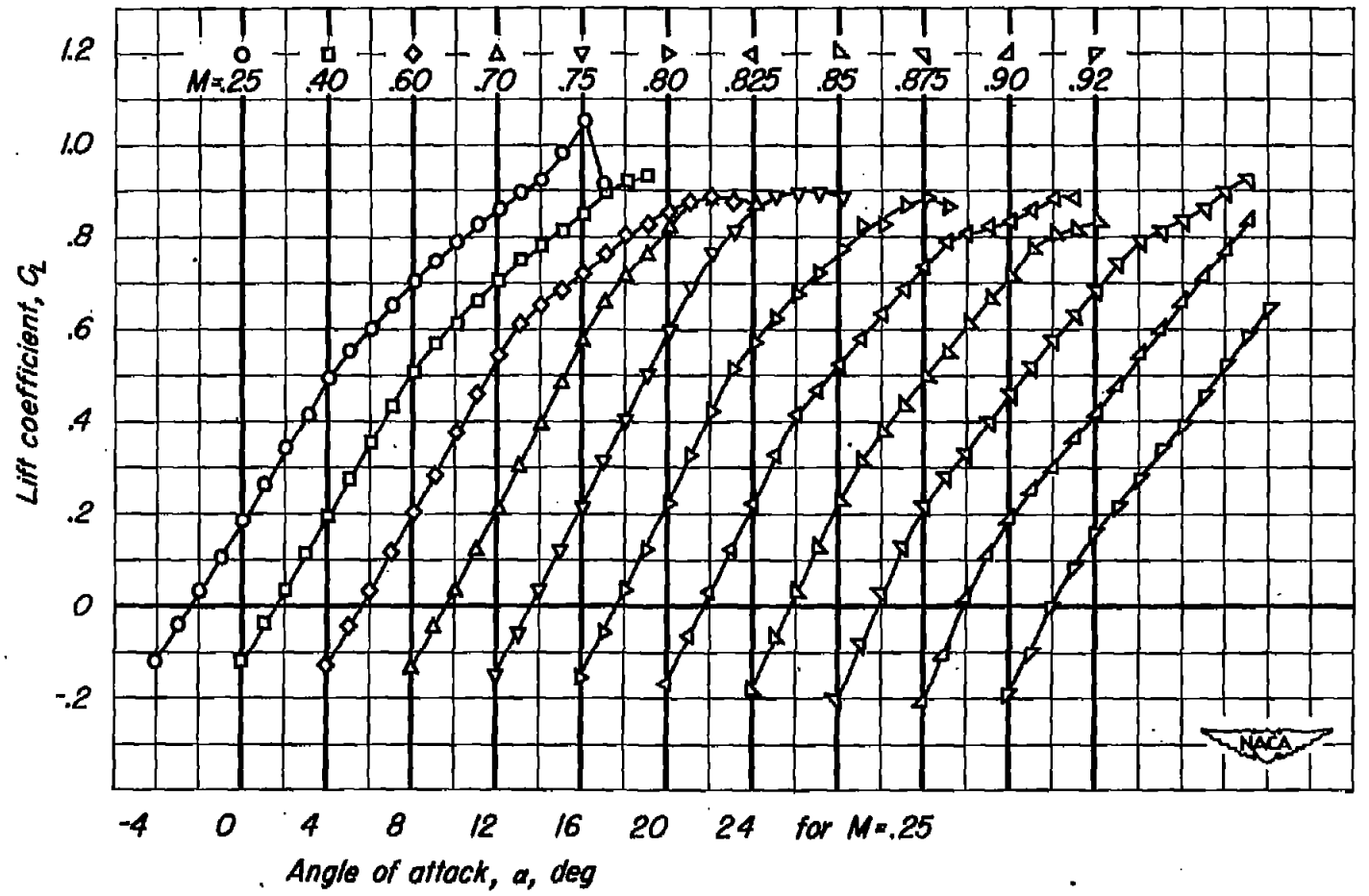

(a) C_L vs α.

Figure 8.– The effect of Mach number on the aerodynamic characteristics. A, 10; airfoil section, NACA 64,A312; R, 2,000,000.

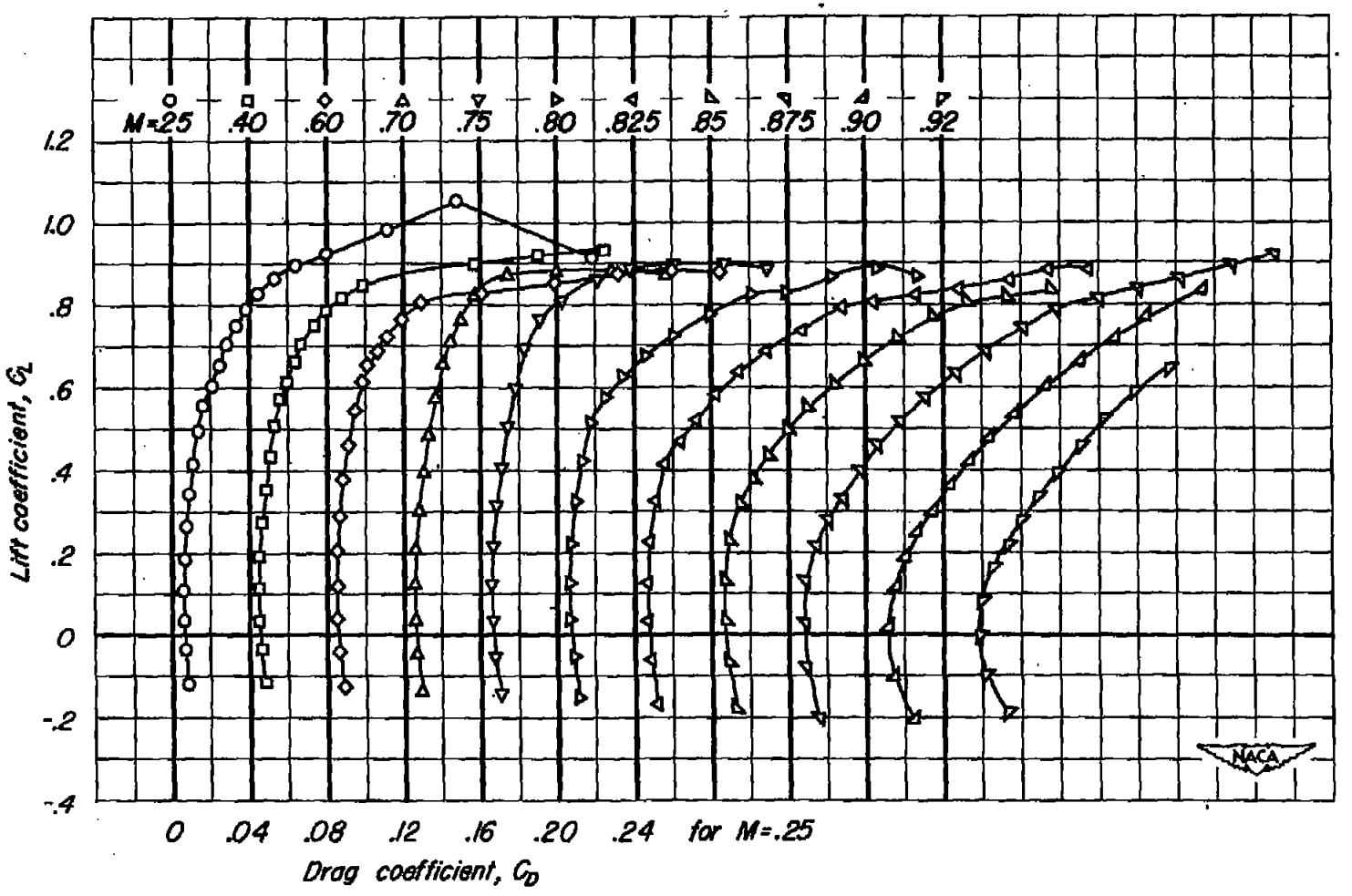

(b) C_L vs C_D.

Figure 8.- Continued.

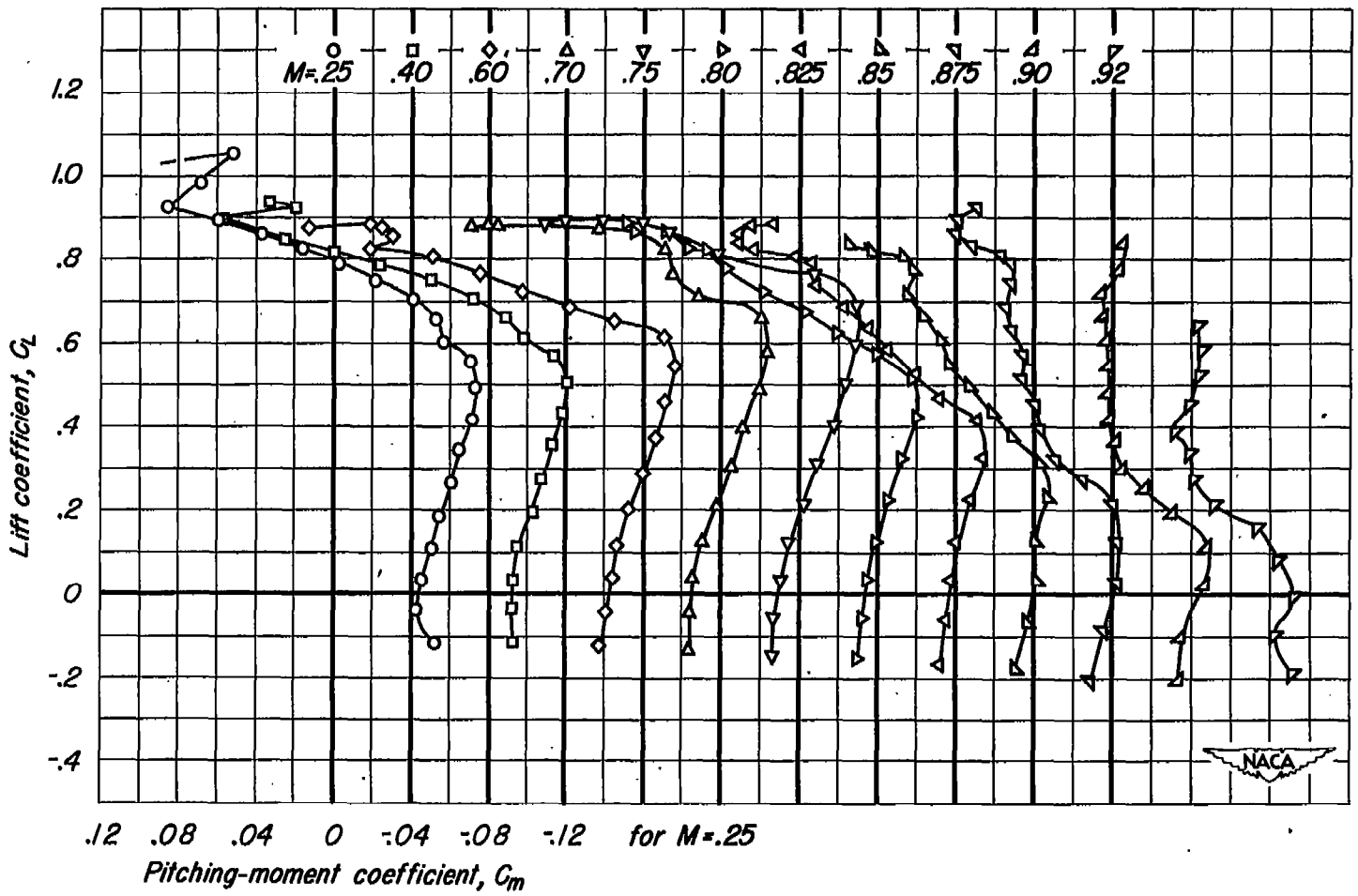

(c) C_L vs C_m.

Figure 8.- Concluded.

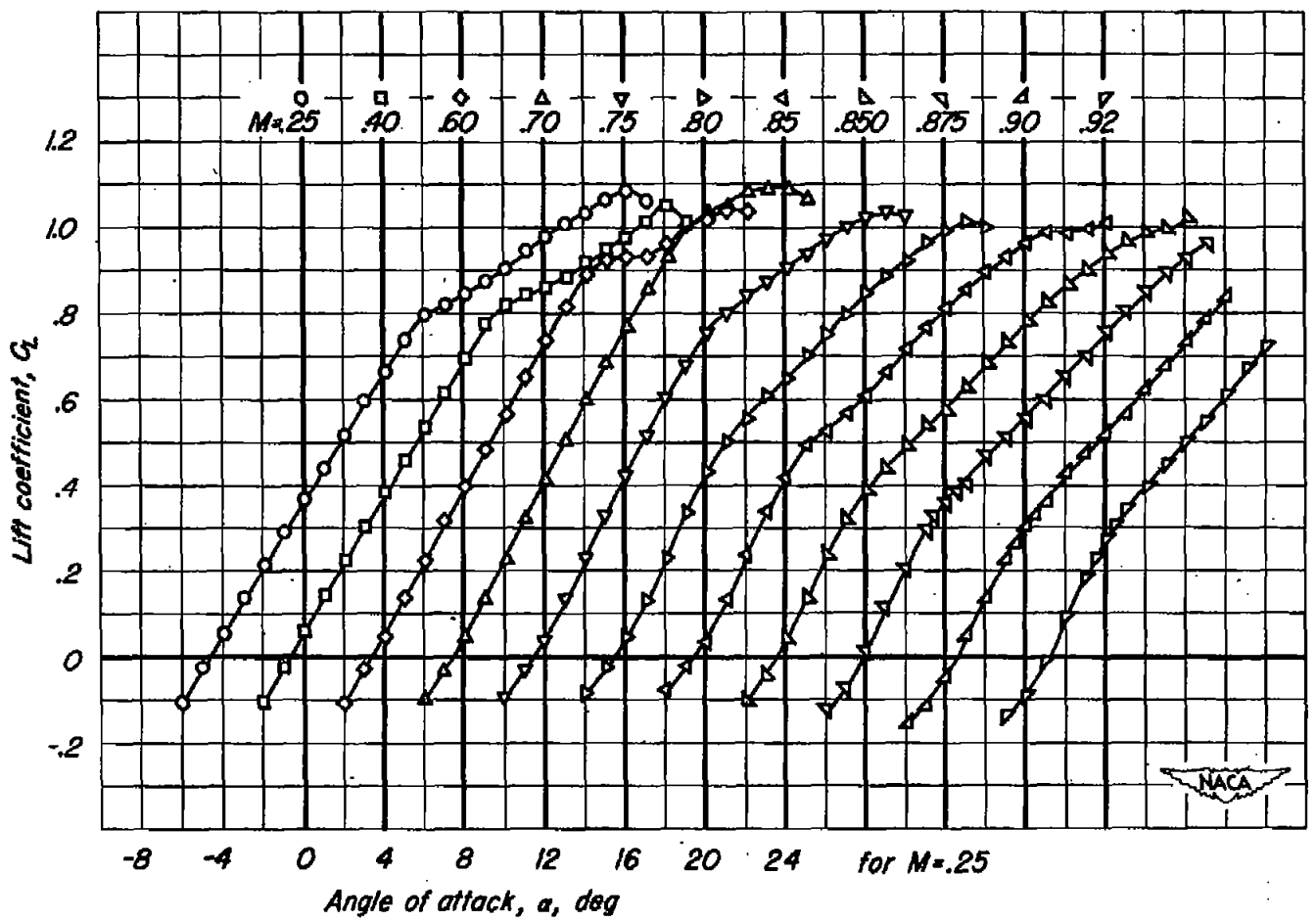

(a) C_L vs α.

Figure 9.- The effect of Mach number on the aerodynamic characteristics. A, 10; airfoil section, NACA 64,A612; R, 2,000,000.

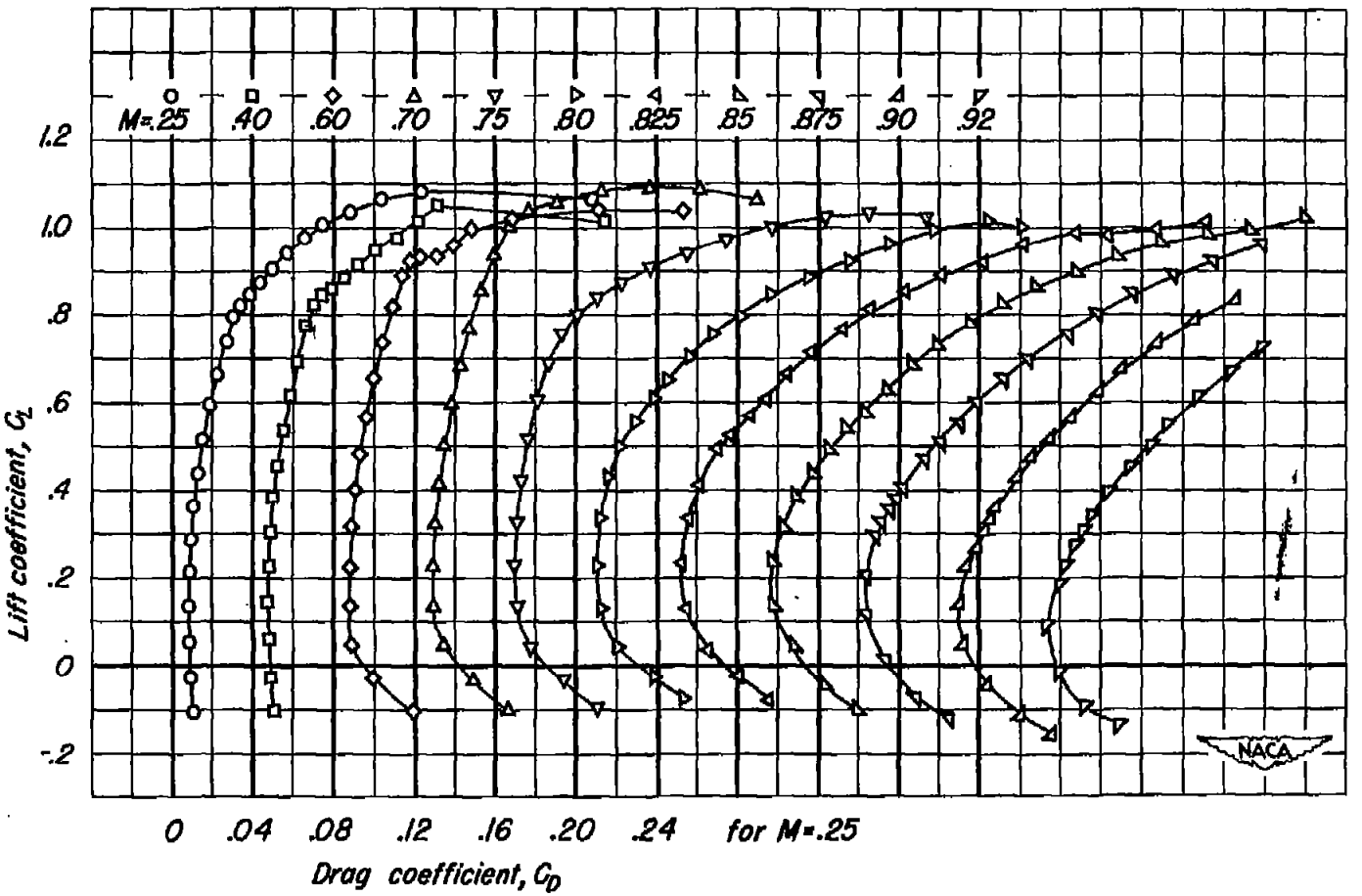

(b) C_L vs C_D.

Figure 9.— Continued.

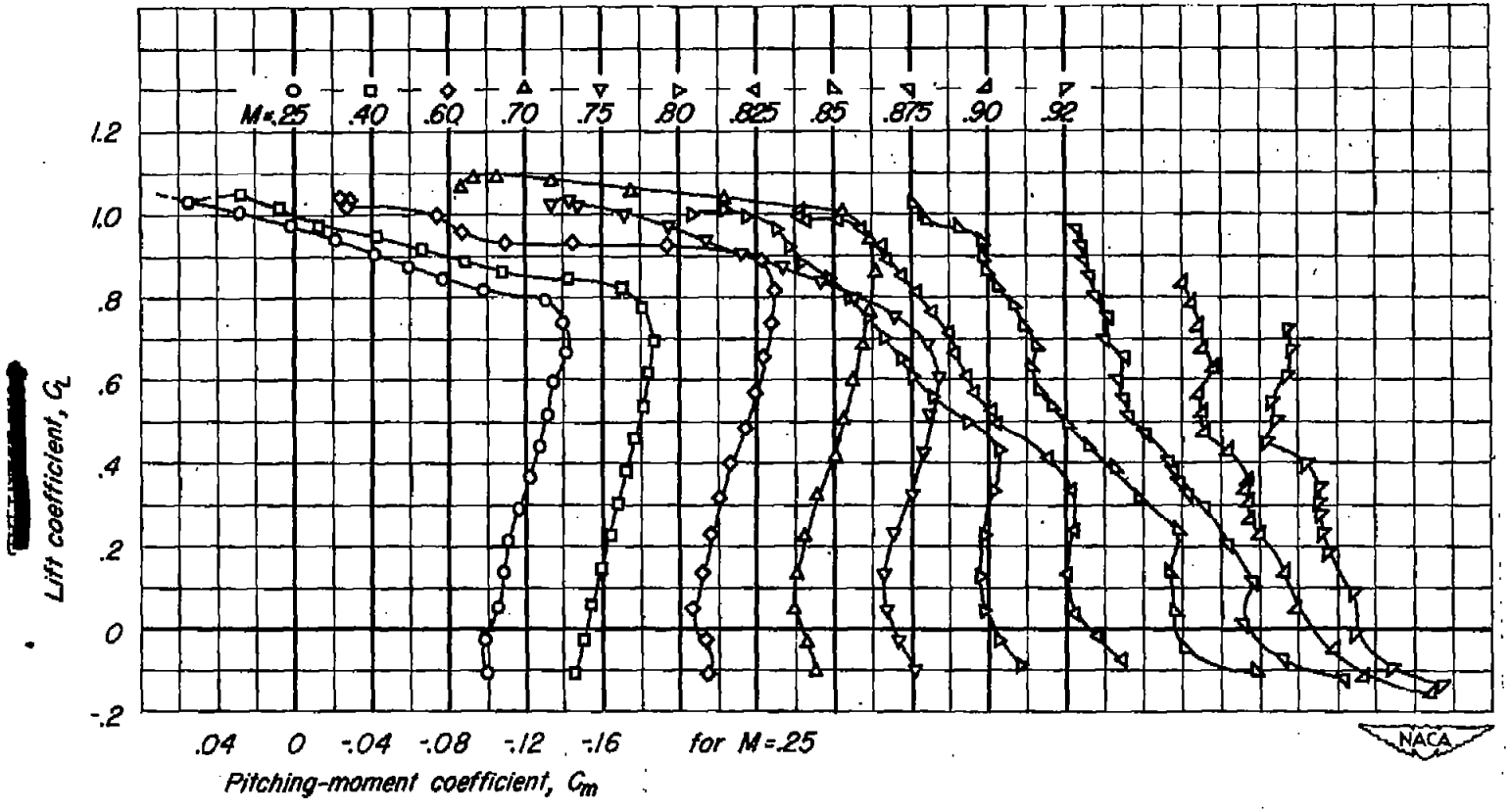

(c) C_L vs C_m.

Figure 9.- Concluded.

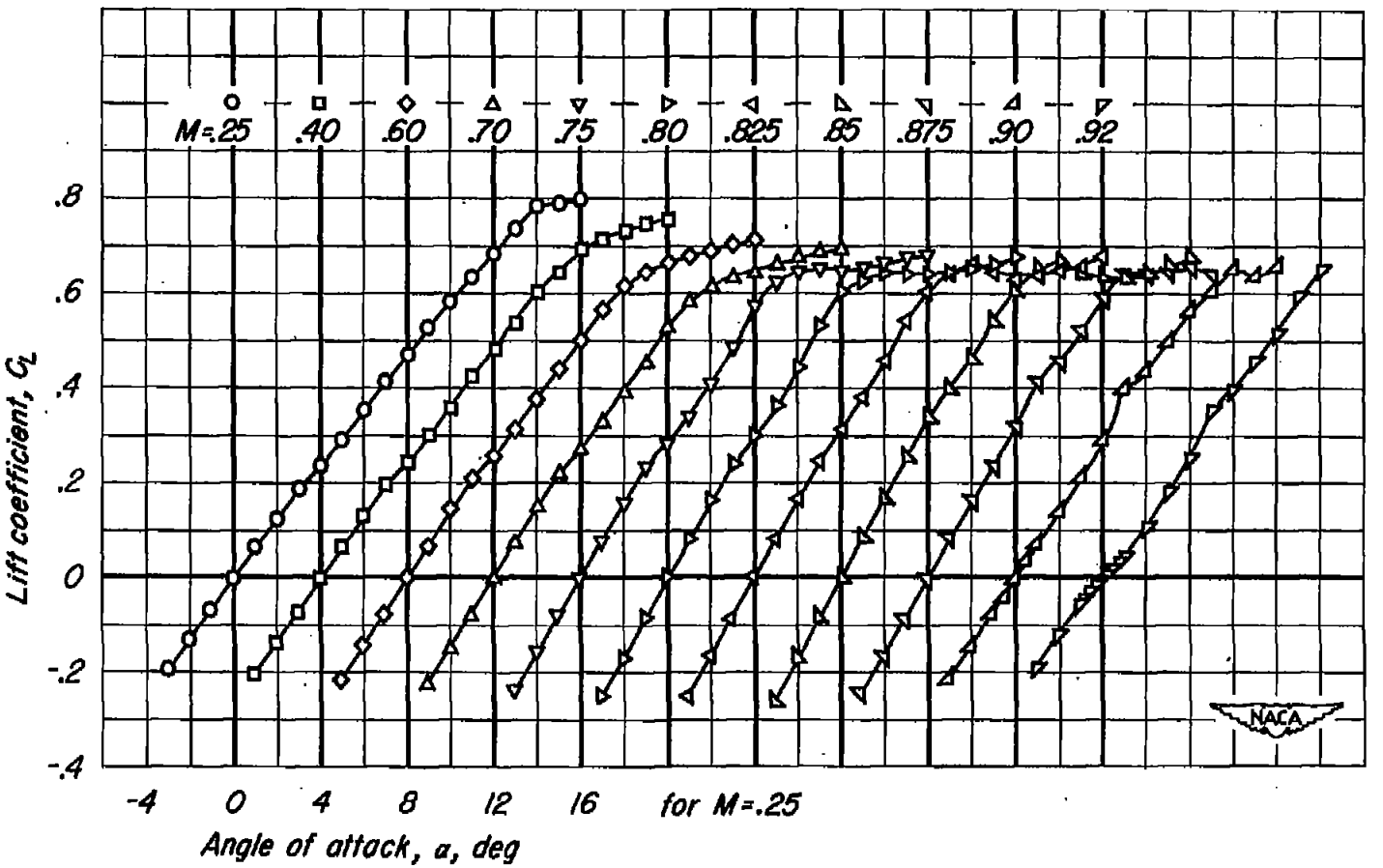

(a) C_L vs α.

Figure 10.– The effect of Mach number on the aerodynamic characteristics. A, 5; airfoil section, NACA 65,A012; R, 2,000,000.

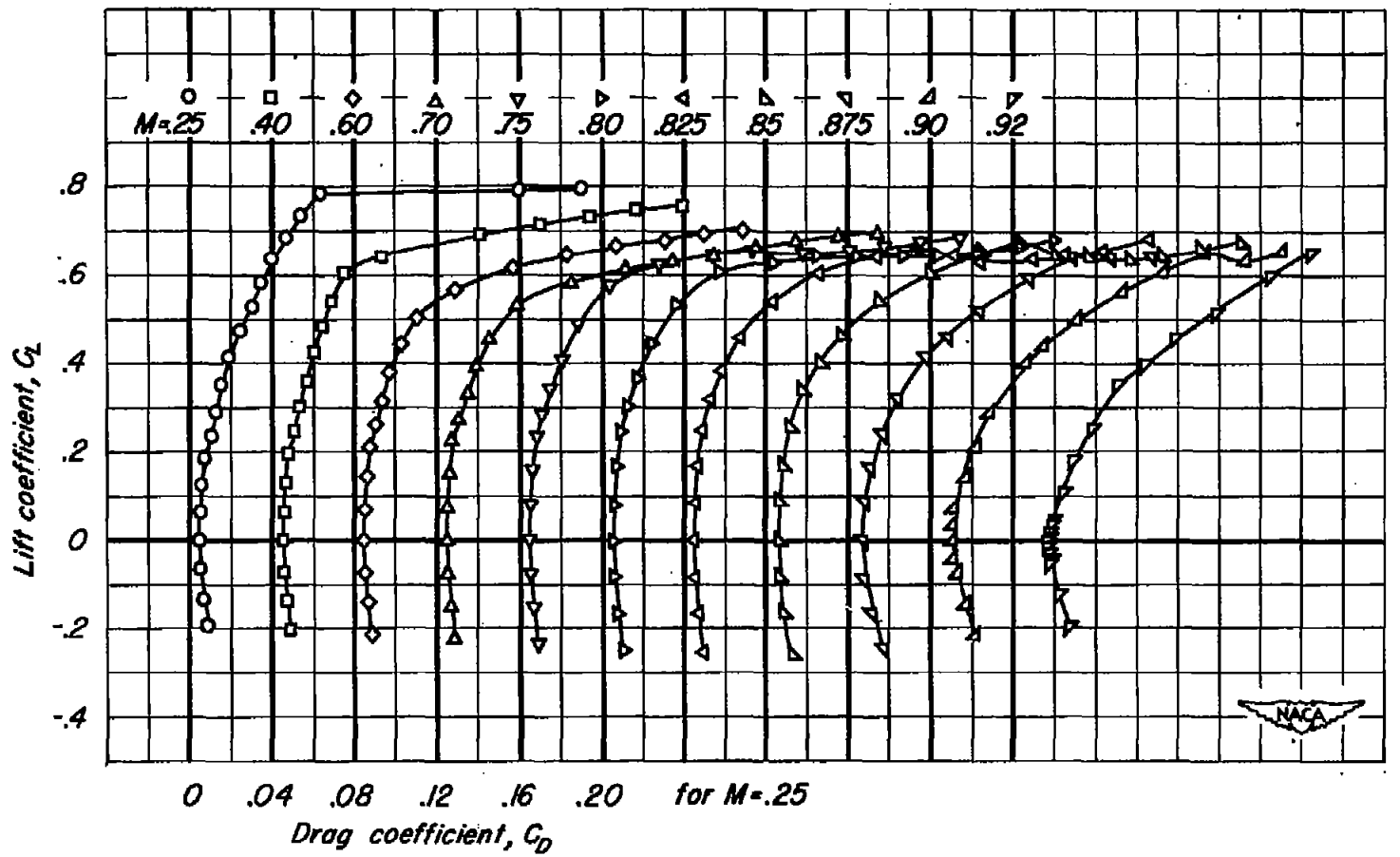

(b) C_L vs C_D.

Figure 10.- Continued.

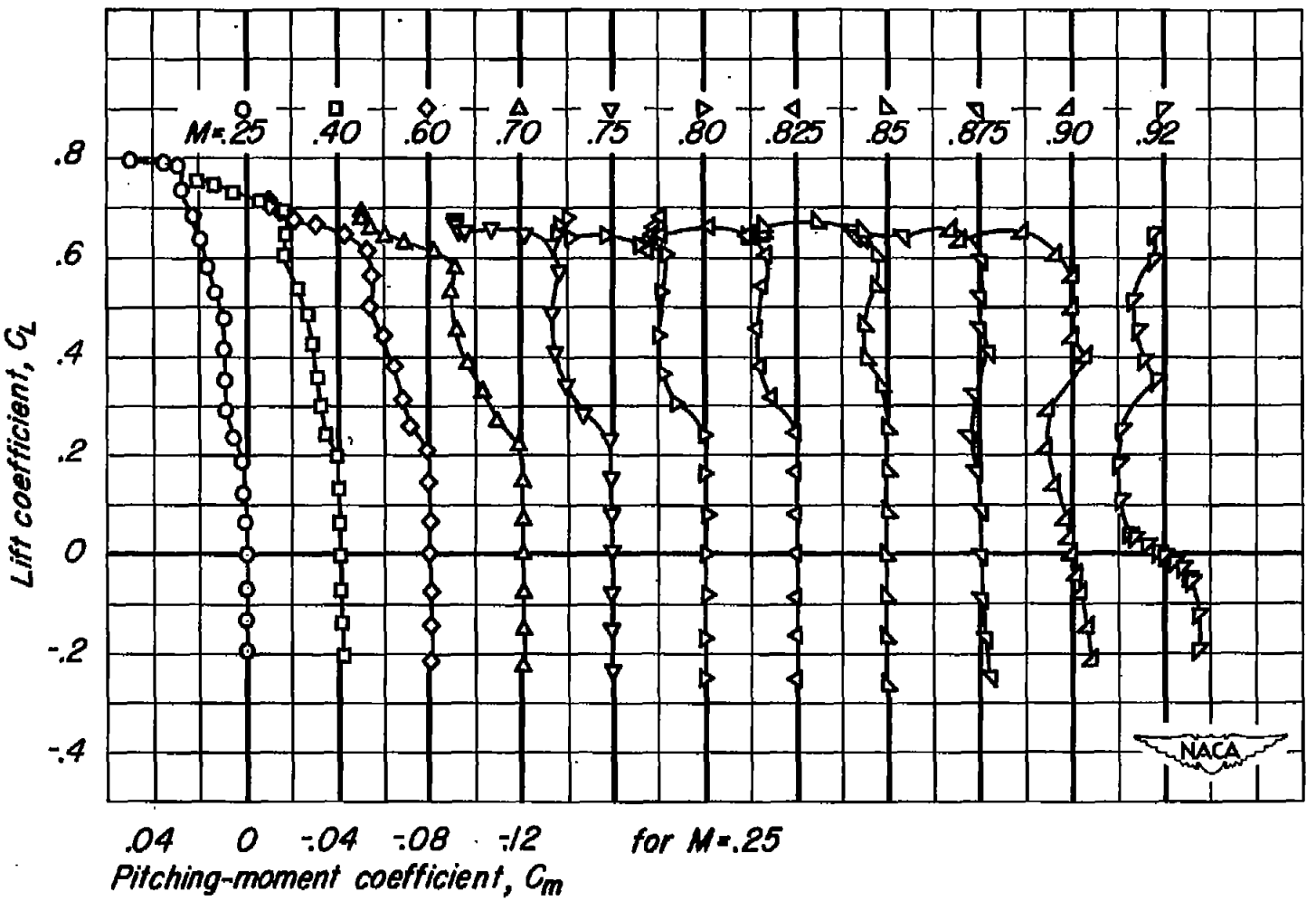

(c) C_L vs C_m.

Figure 10.— Concluded.

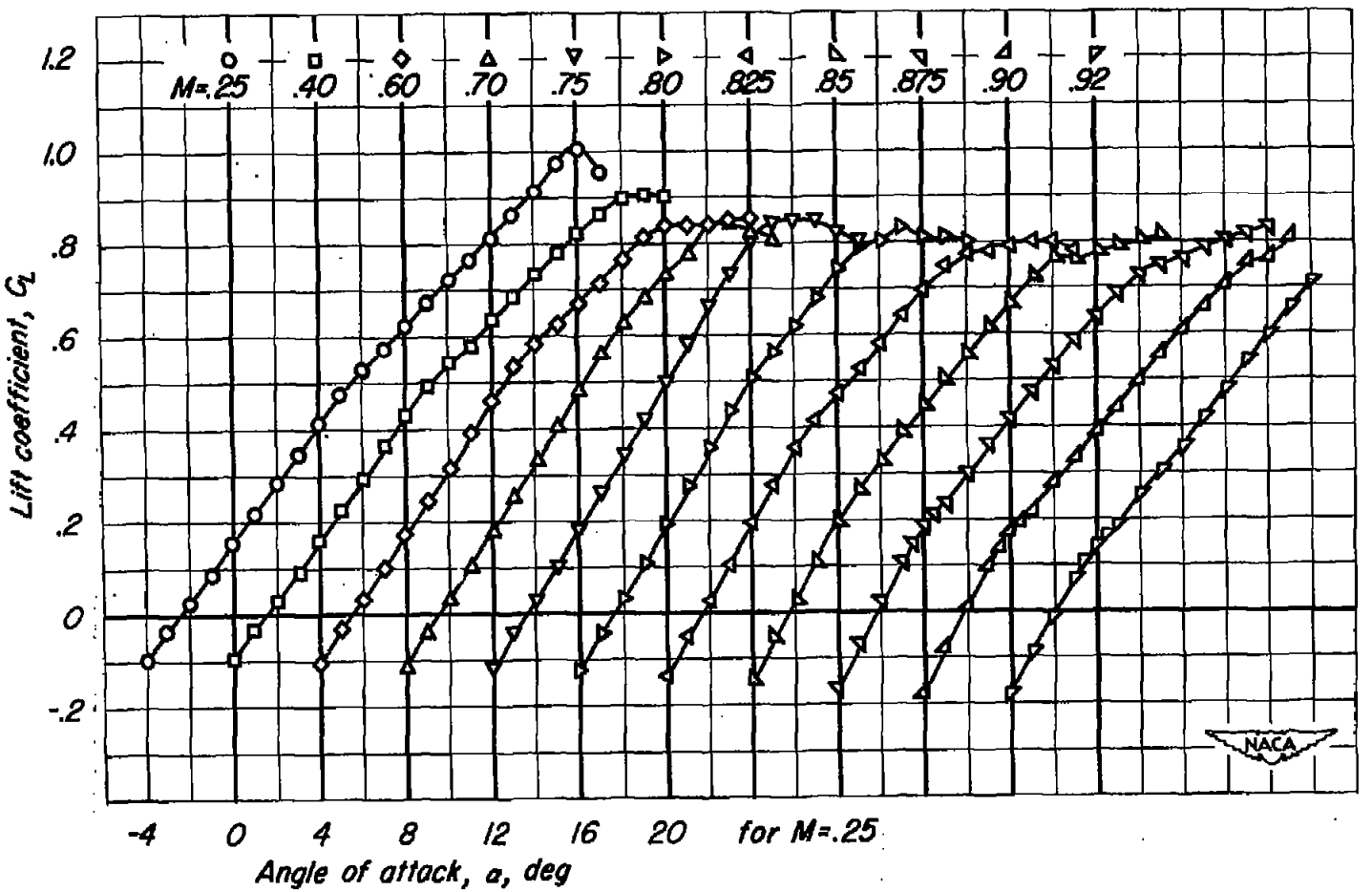

(a) C_L vs α.

Figure 11.– The effect of Mach number on the aerodynamic characteristics. A, 5; airfoil section, NACA 64,A312; R, 2,000,000.

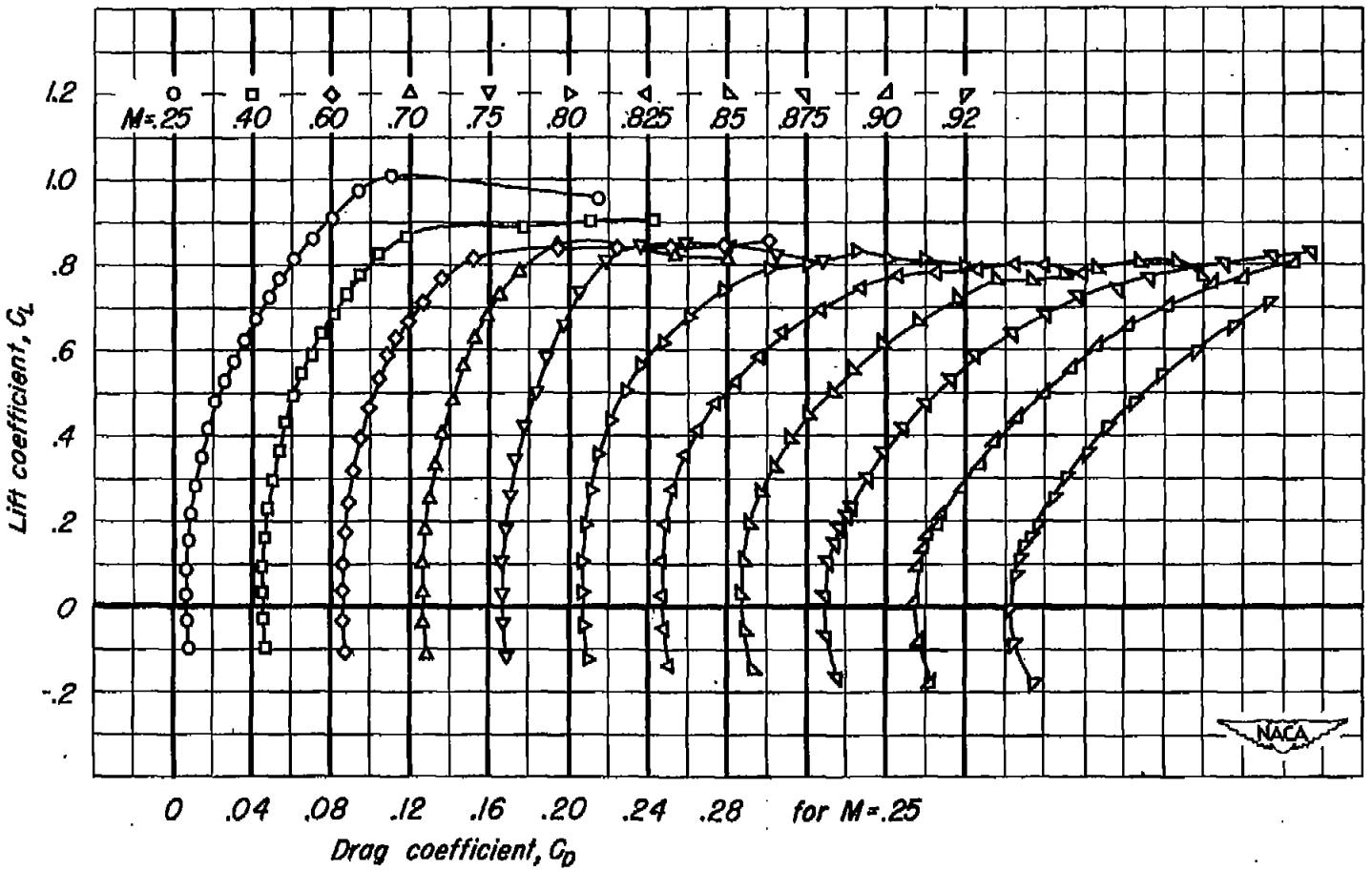

(b) C_L vs C_D.

Figure 11.– Continued.

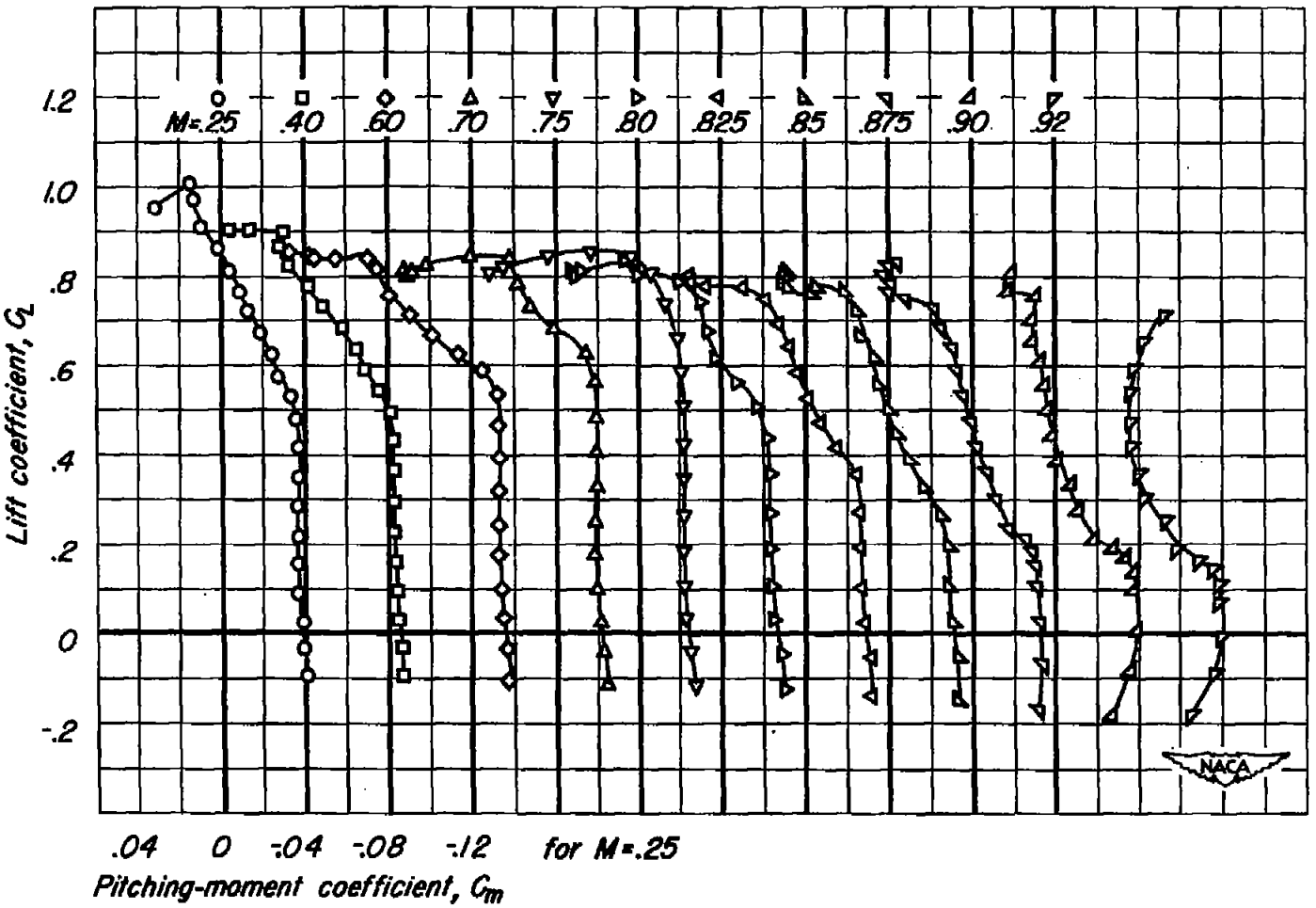

(c) C_L vs C_m.

Figure 11.- Concluded.

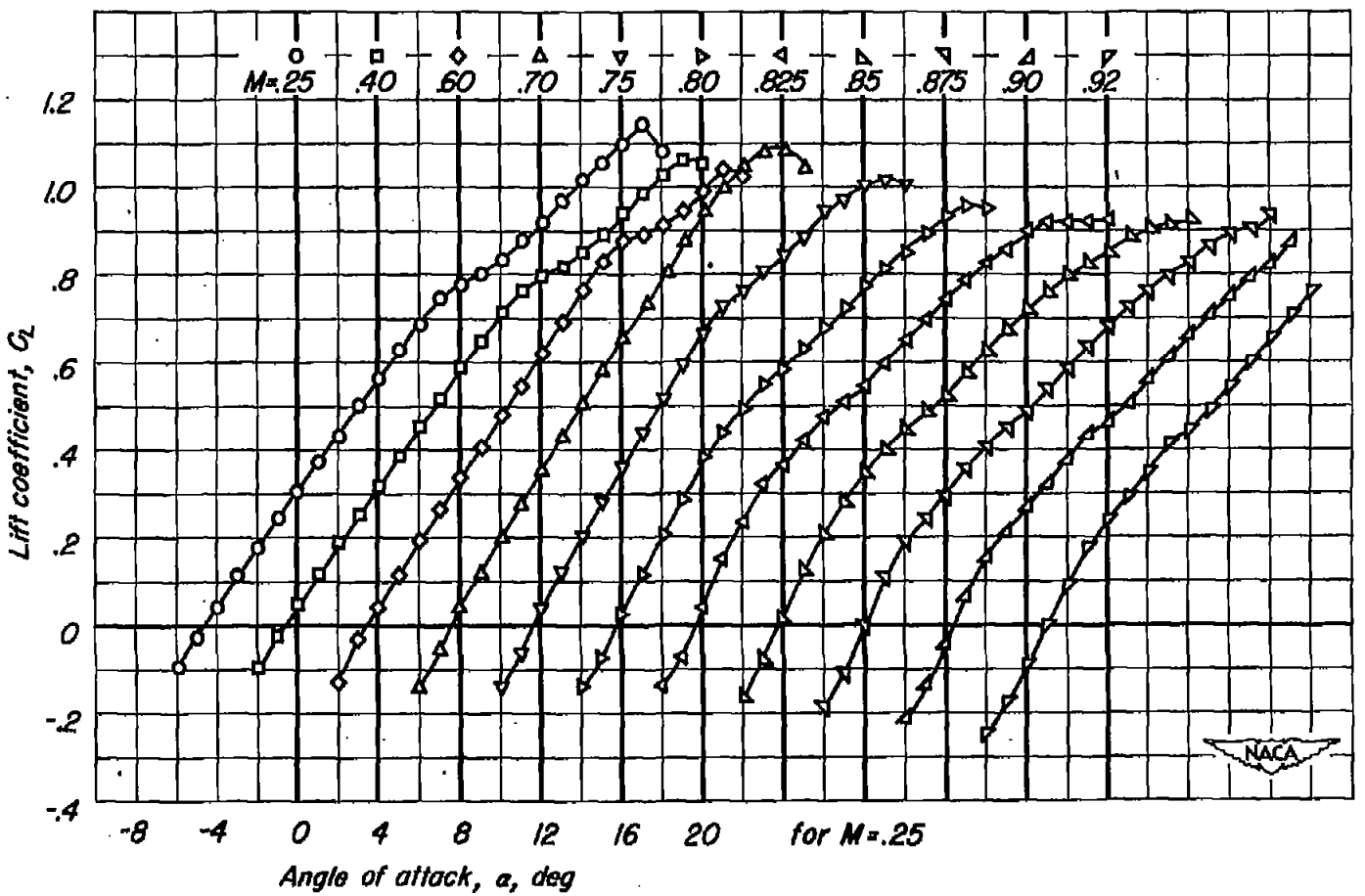

(a) C_L vs α.

Figure 12.– The effect of Mach number on the aerodynamic characteristics. A, 5; airfoil section, NACA 64,A612; R, 2,000,000.

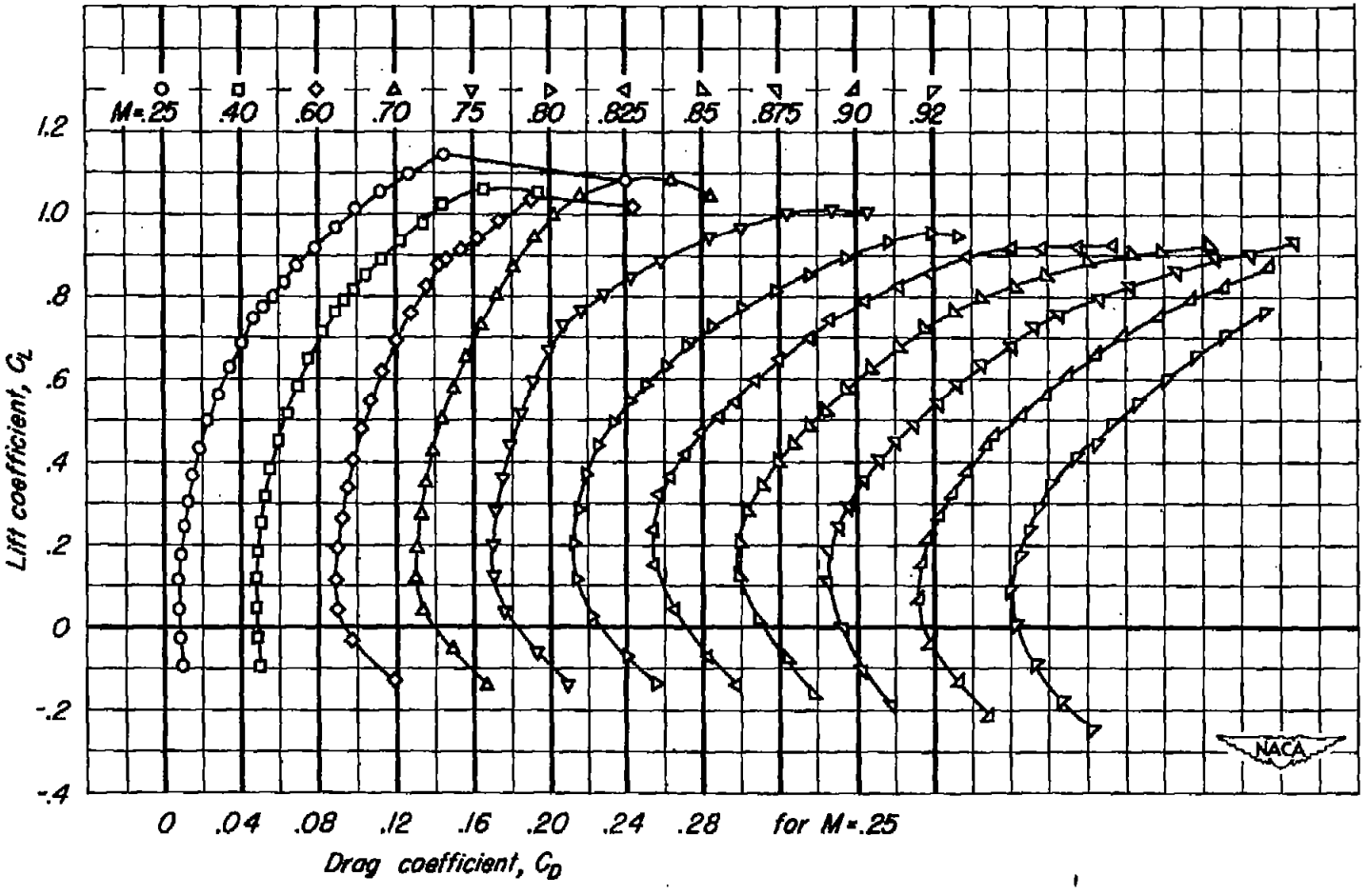

(b) C_L vs C_D.

Figure 12.- Continued.

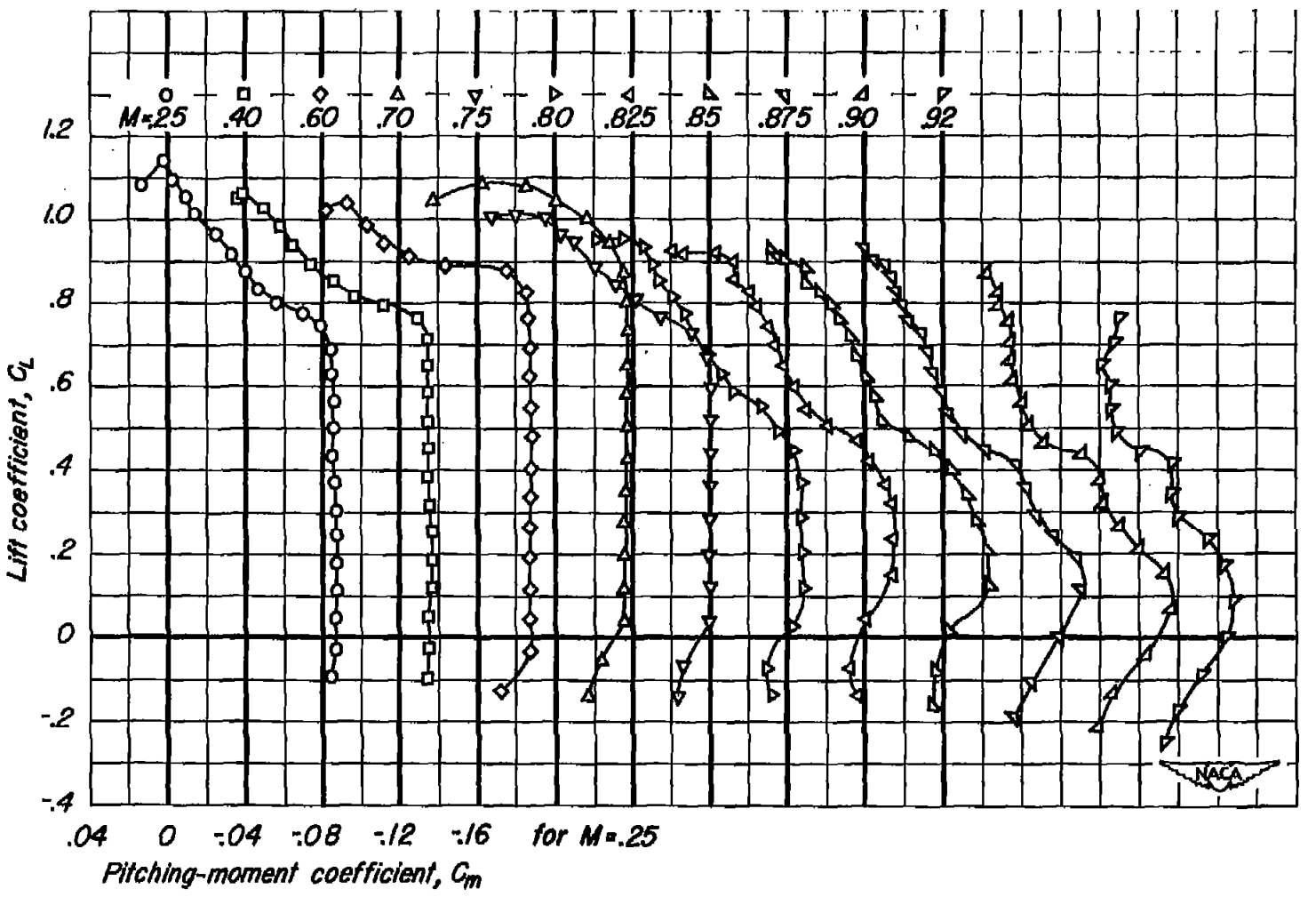

(c) C_L vs C_m.

Figure 12.- Concluded.

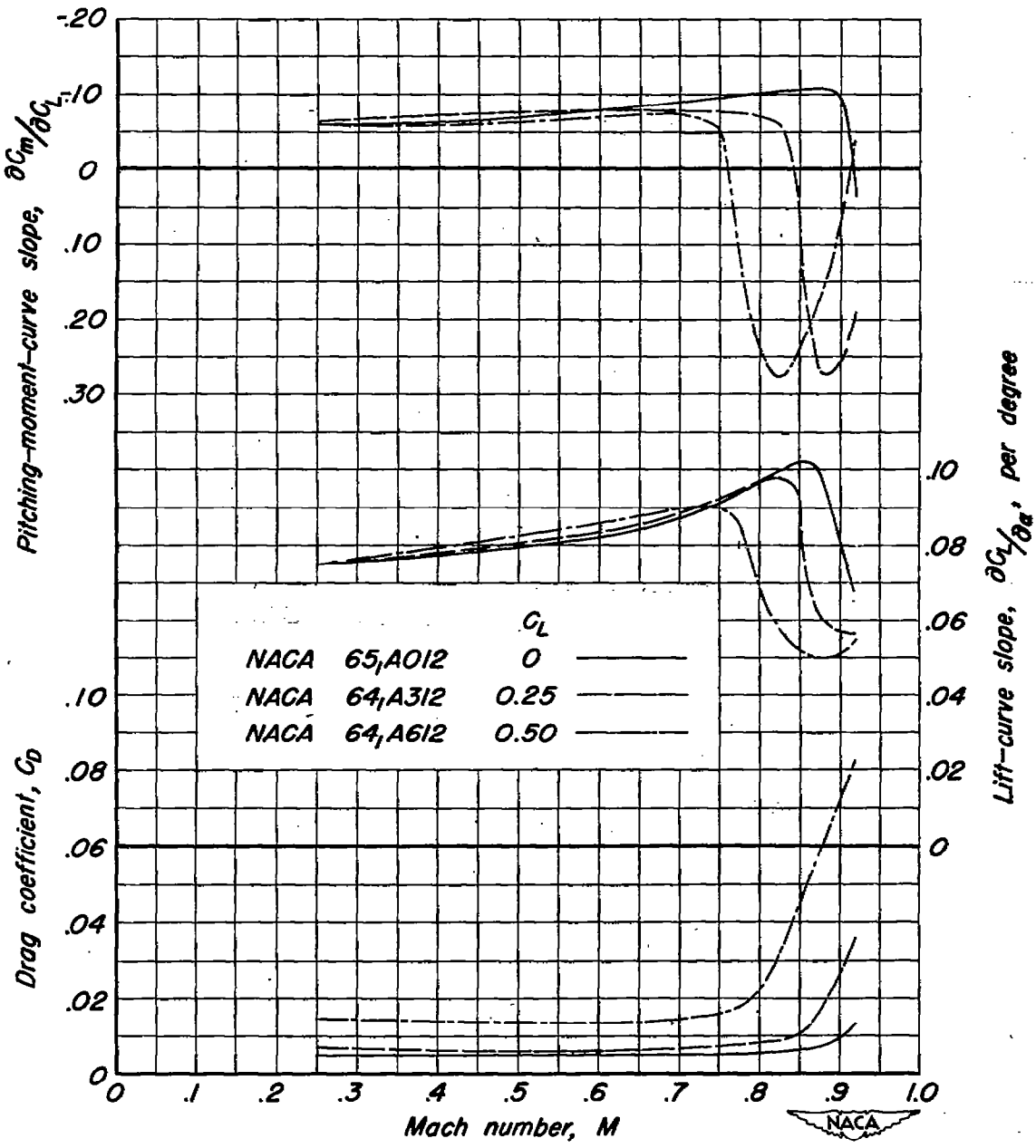

(a) A, 10.

Figure 13.— The variations of the drag coefficient, the lift-curve slope, and the pitching-moment-curve slope with Mach number.

[redacted]

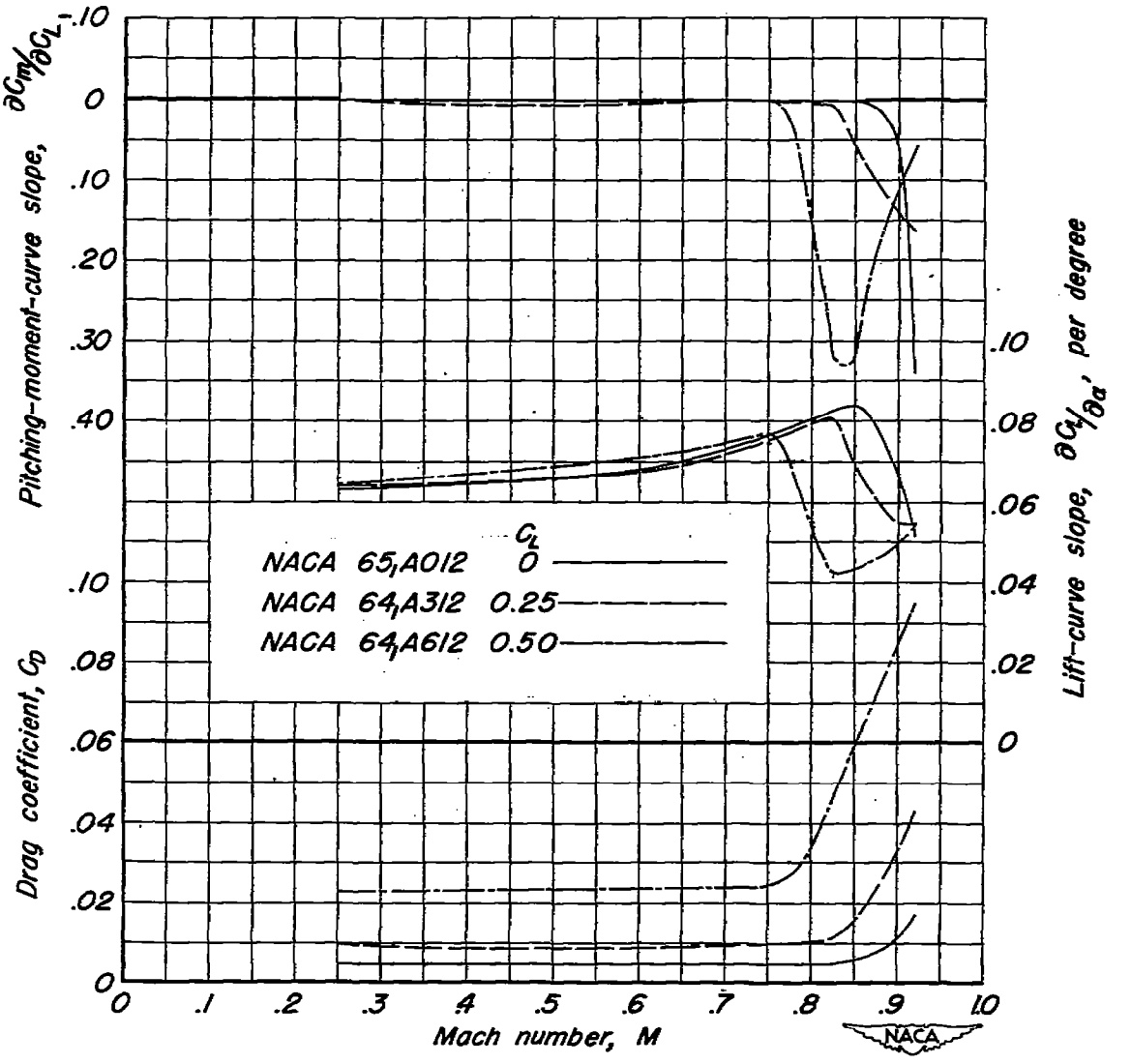

(b) A, 5.

Figure 13.— Concluded.

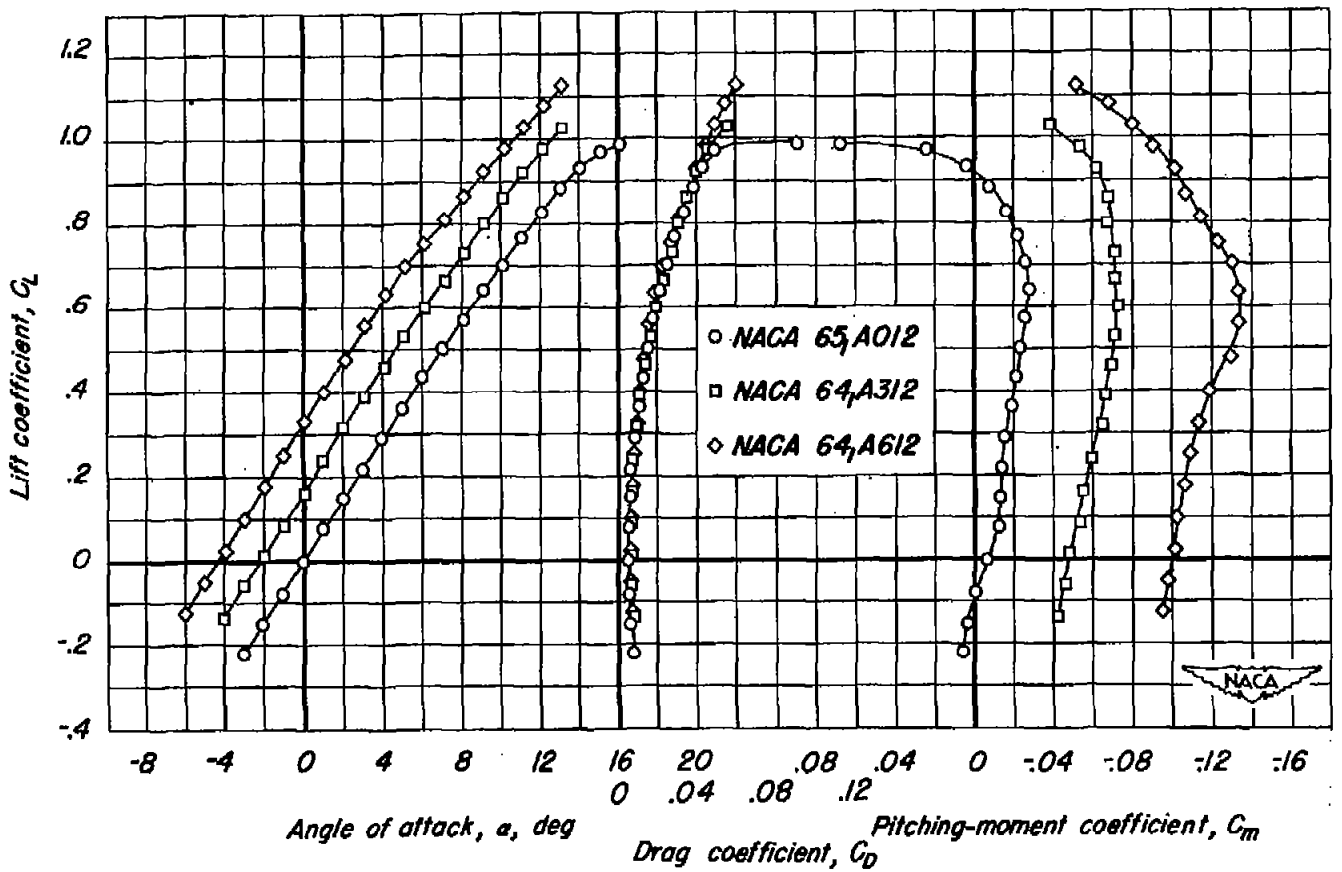

(a) A, 10.

Figure 14.— The low-speed aerodynamic characteristics of several wings having various amounts of camber. R, 10,000,000; M, 0.25.

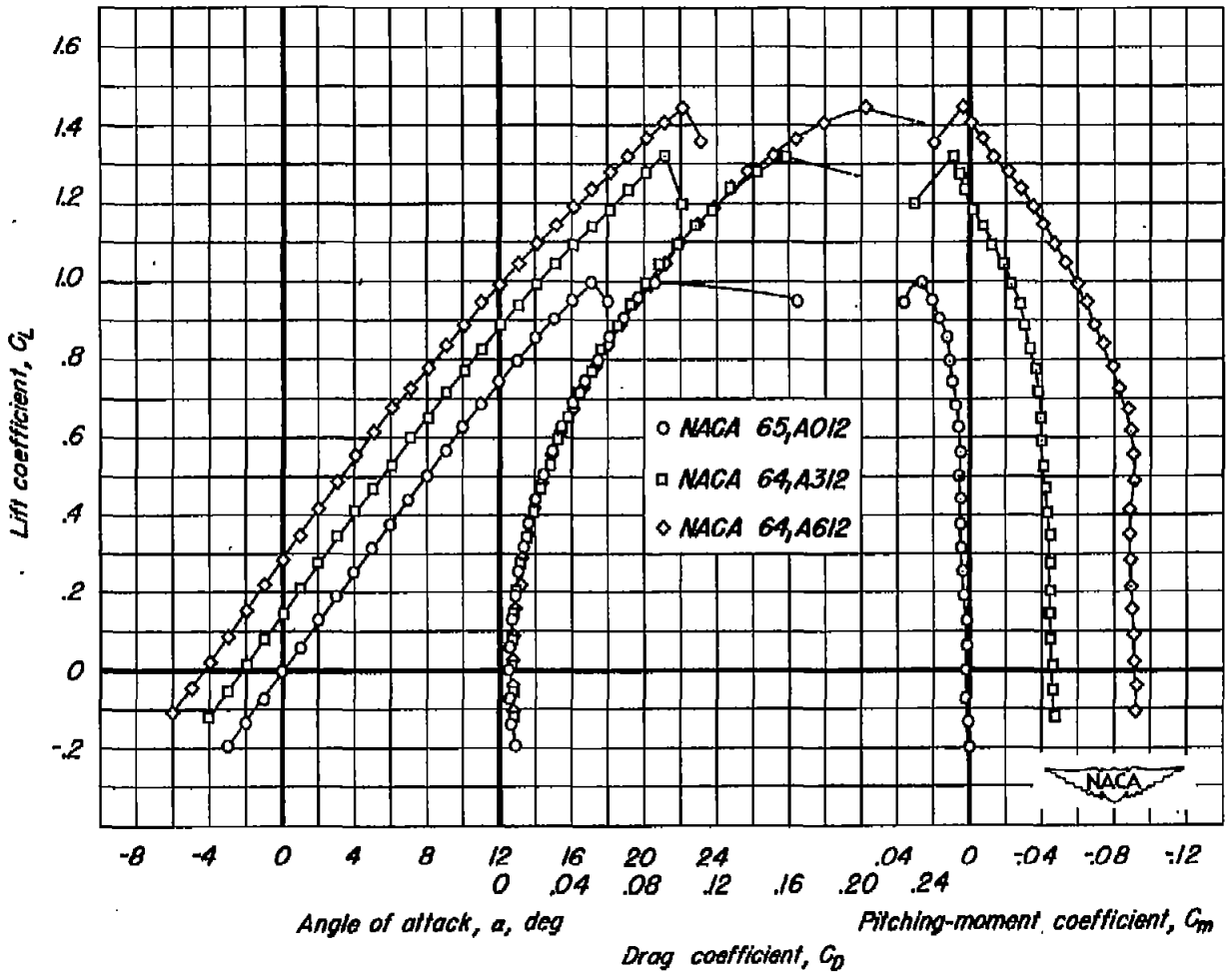

(b) A, 5.

Figure 14.- Concluded.

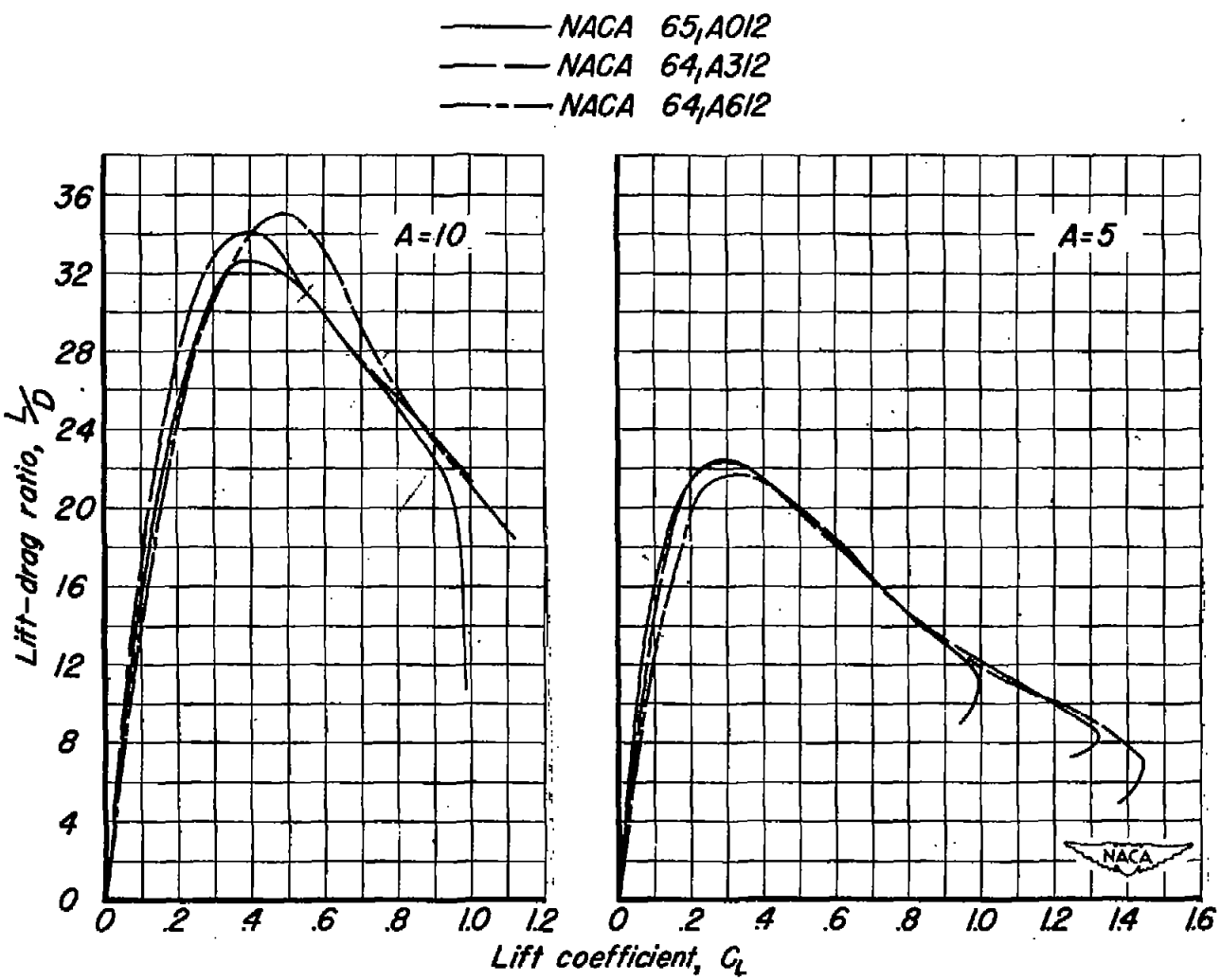

Figure 15.— The variation of lift-drag ratio with lift coefficient of several wings having various amounts of camber. R, 10,000,000; M, 0.25.

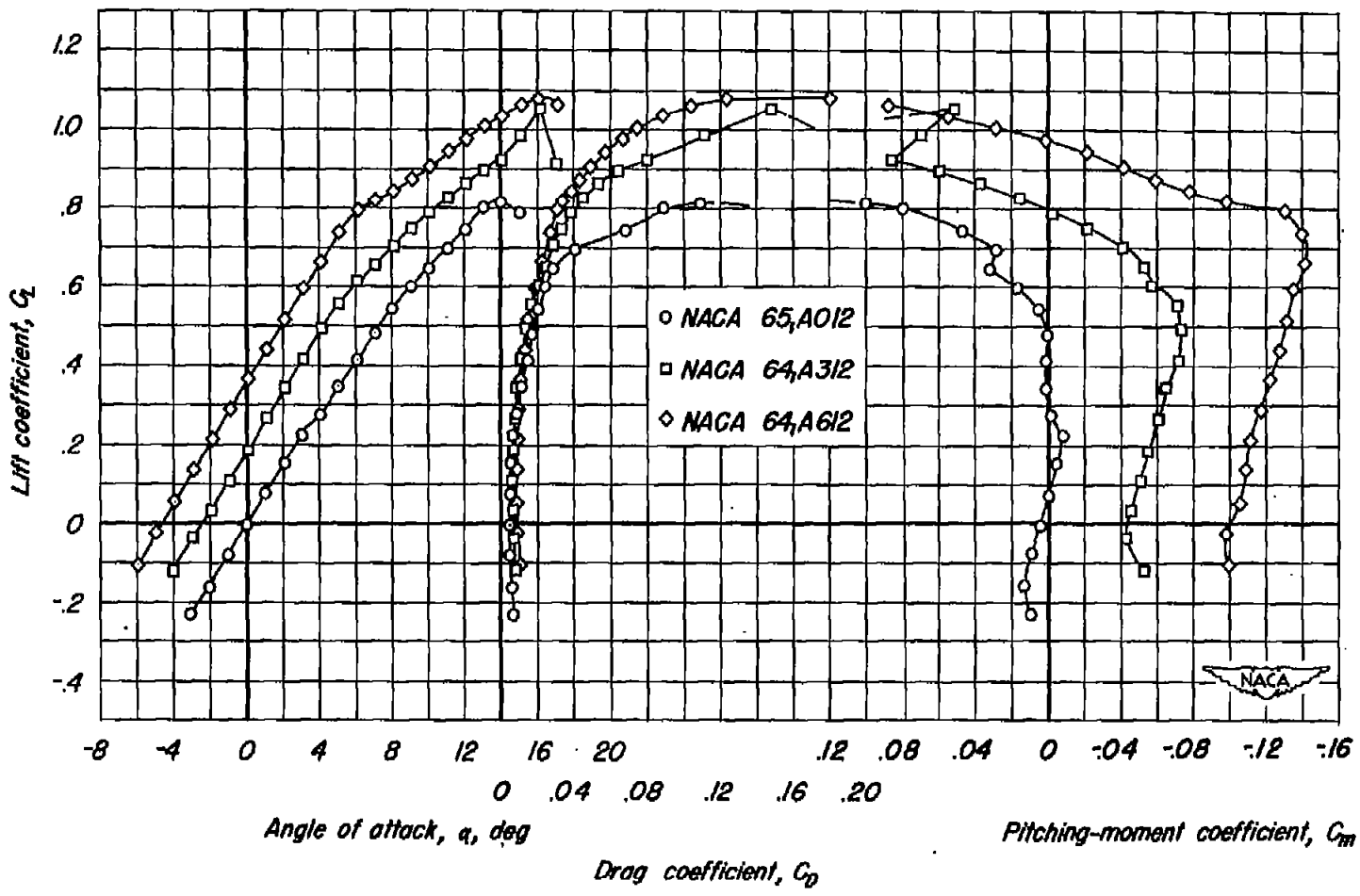

(a) A, 10.

Figure 16.- The low-speed aerodynamic characteristics of several wings having various amounts of camber. R, 2,000,000; M, 0.25.

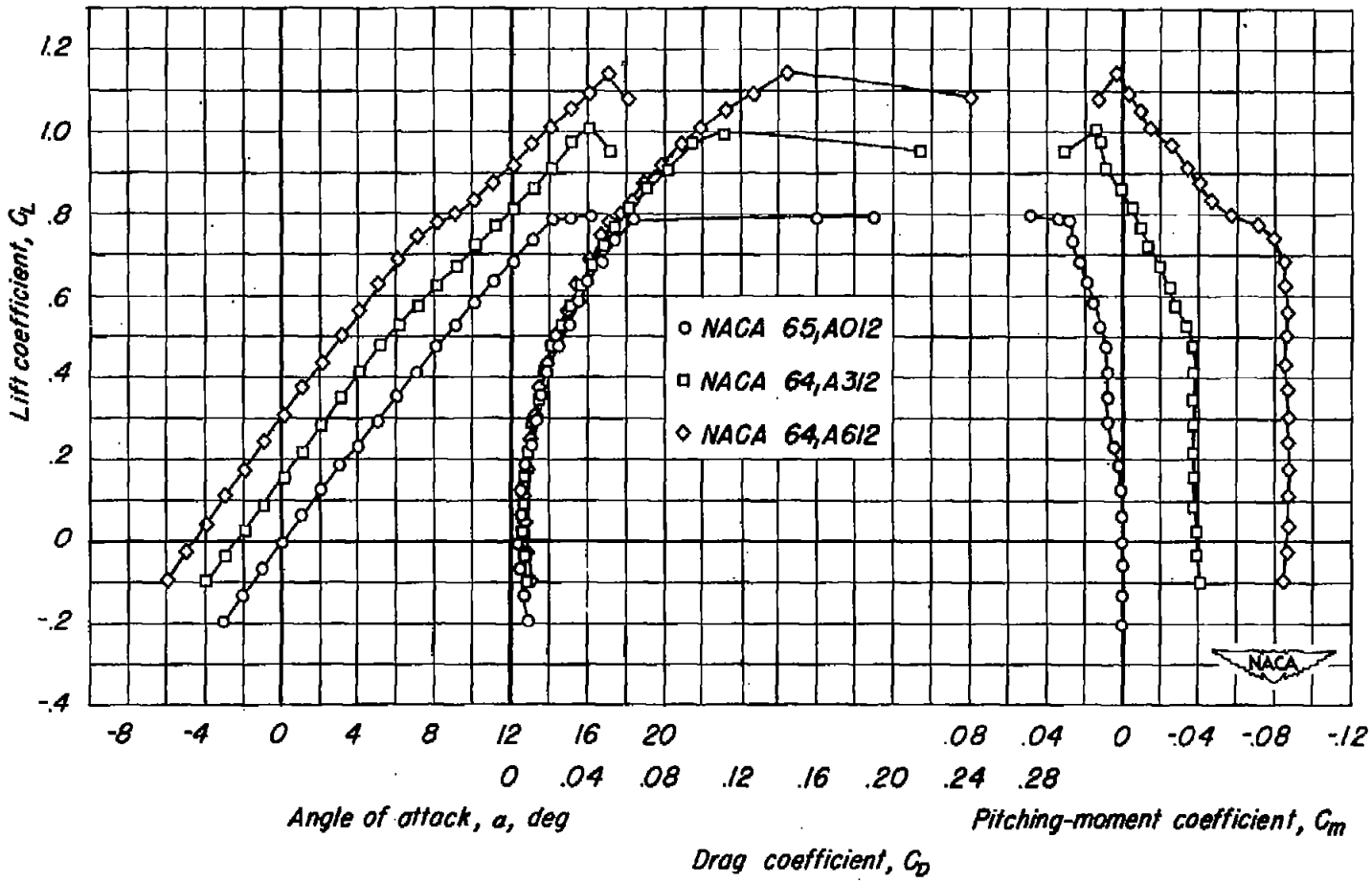

(b) A, 5.

Figure 16.- Concluded.

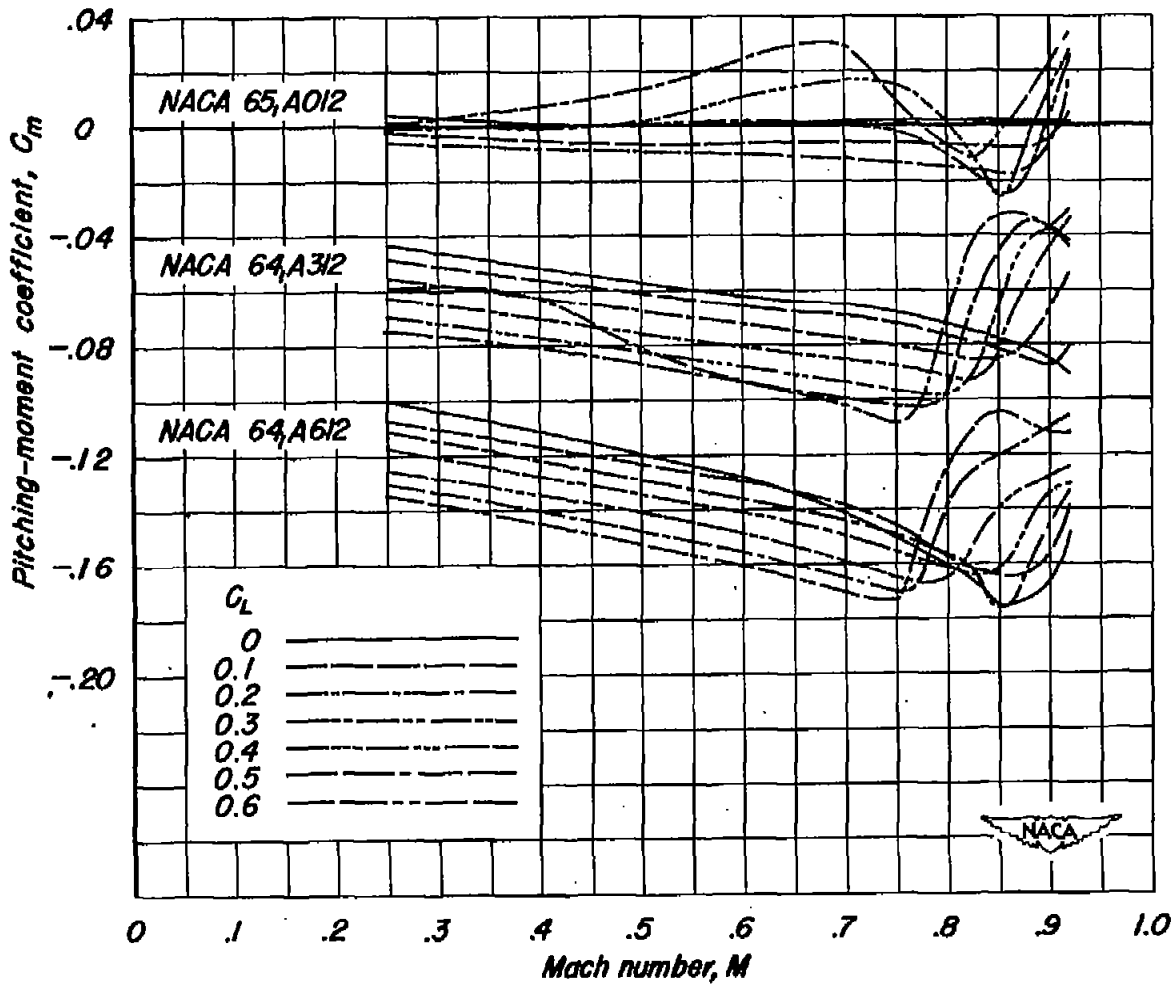

(a) A, 10.

Figure 17.- The variation of pitching-moment coefficient with Mach number. R, 2,000,000.

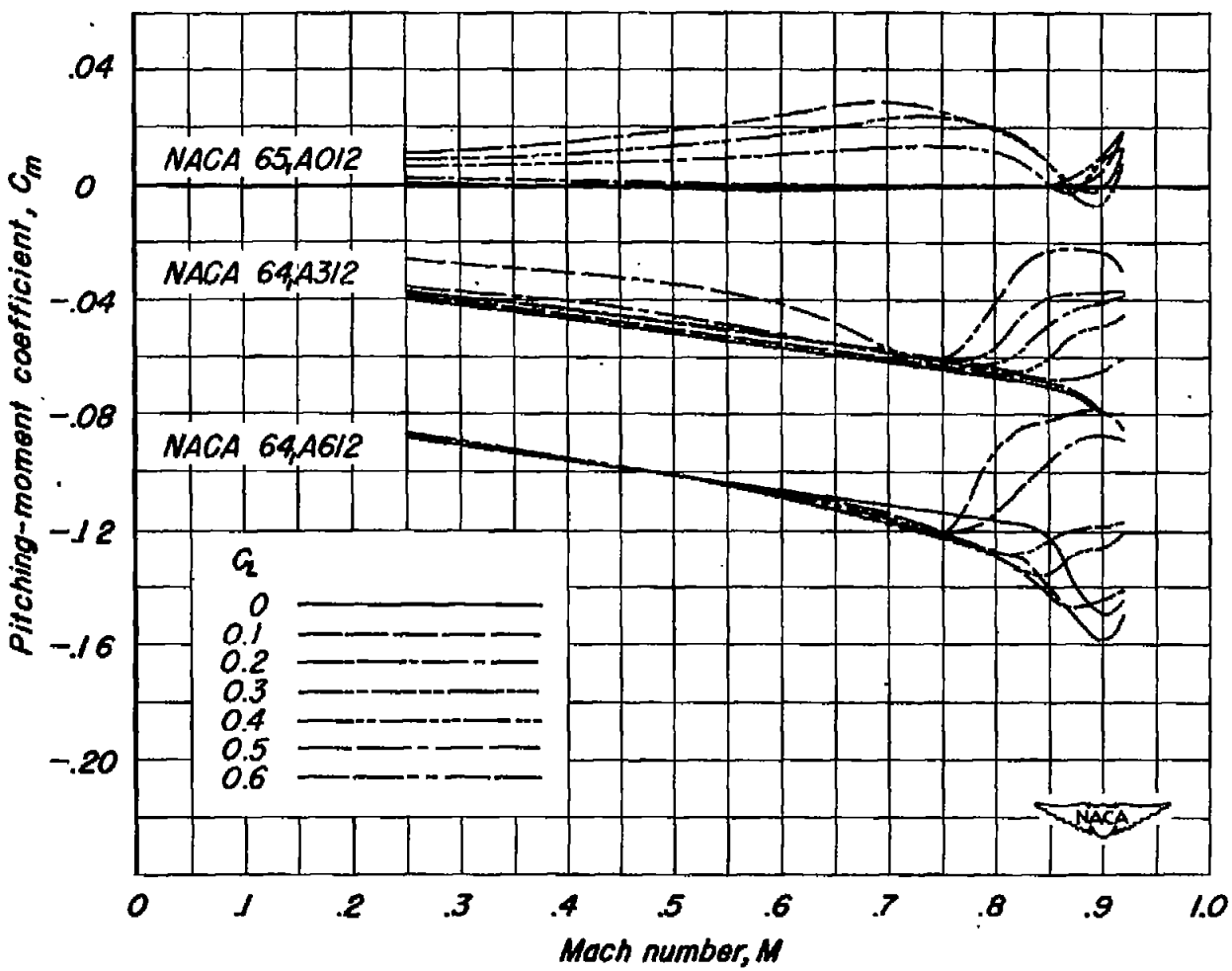

(b) A, 5.

Figure 17.- Concluded.

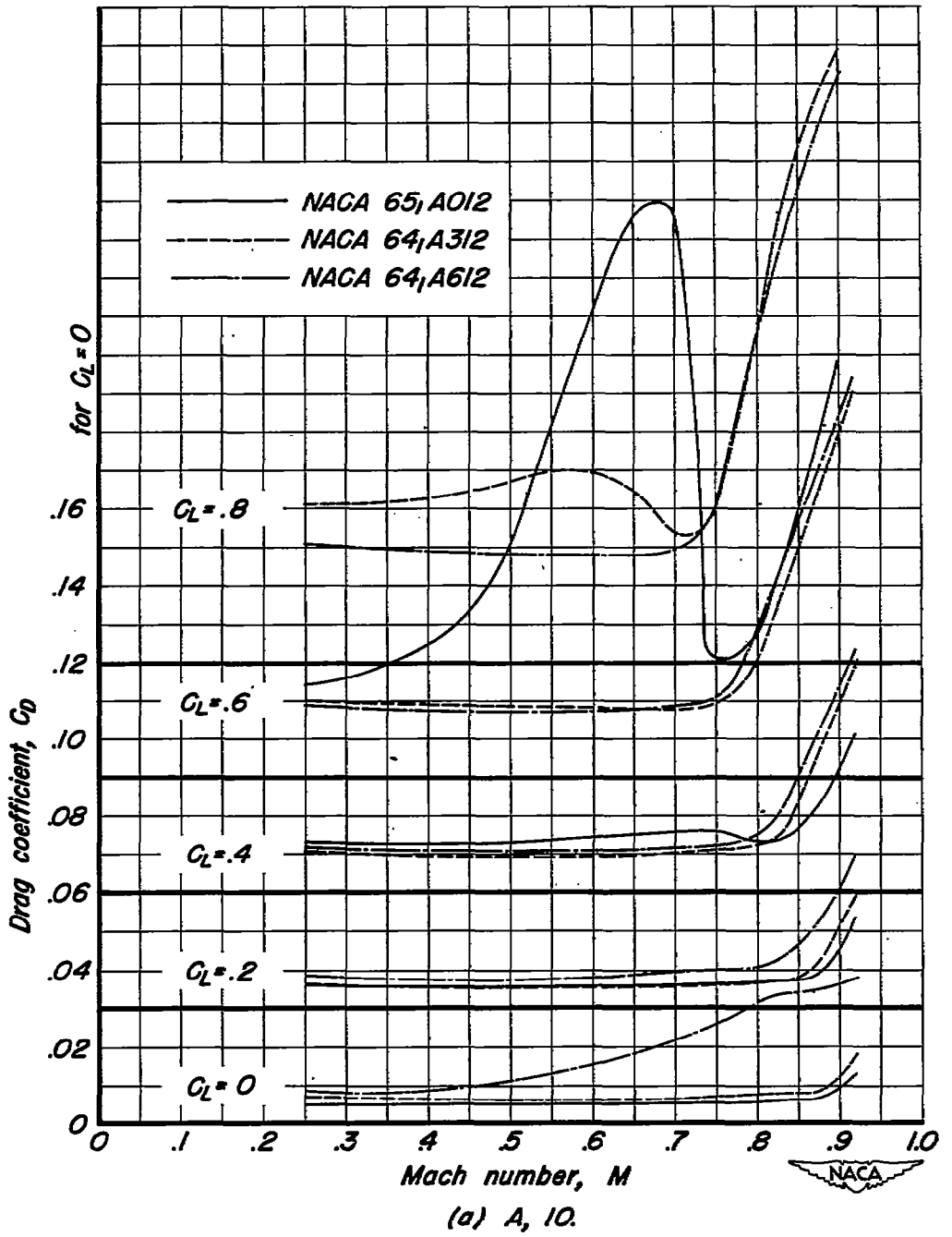

(a) A, 10.

Figure 18.– The variation of drag coefficient with Mach number for several values of lift coefficient. R, 2,000,000.

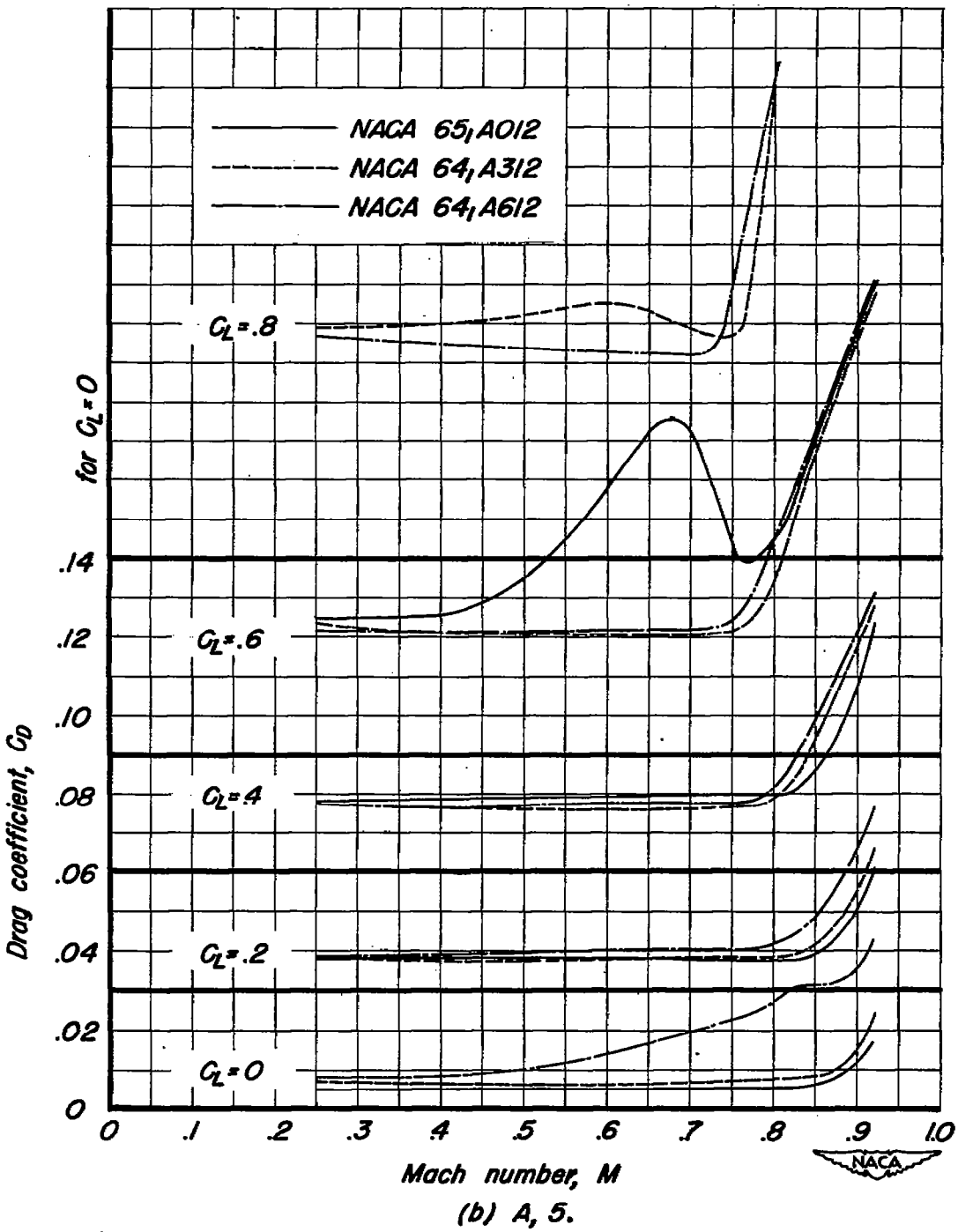

(b) A, 5.

Figure 18.– Concluded.

[redacted]

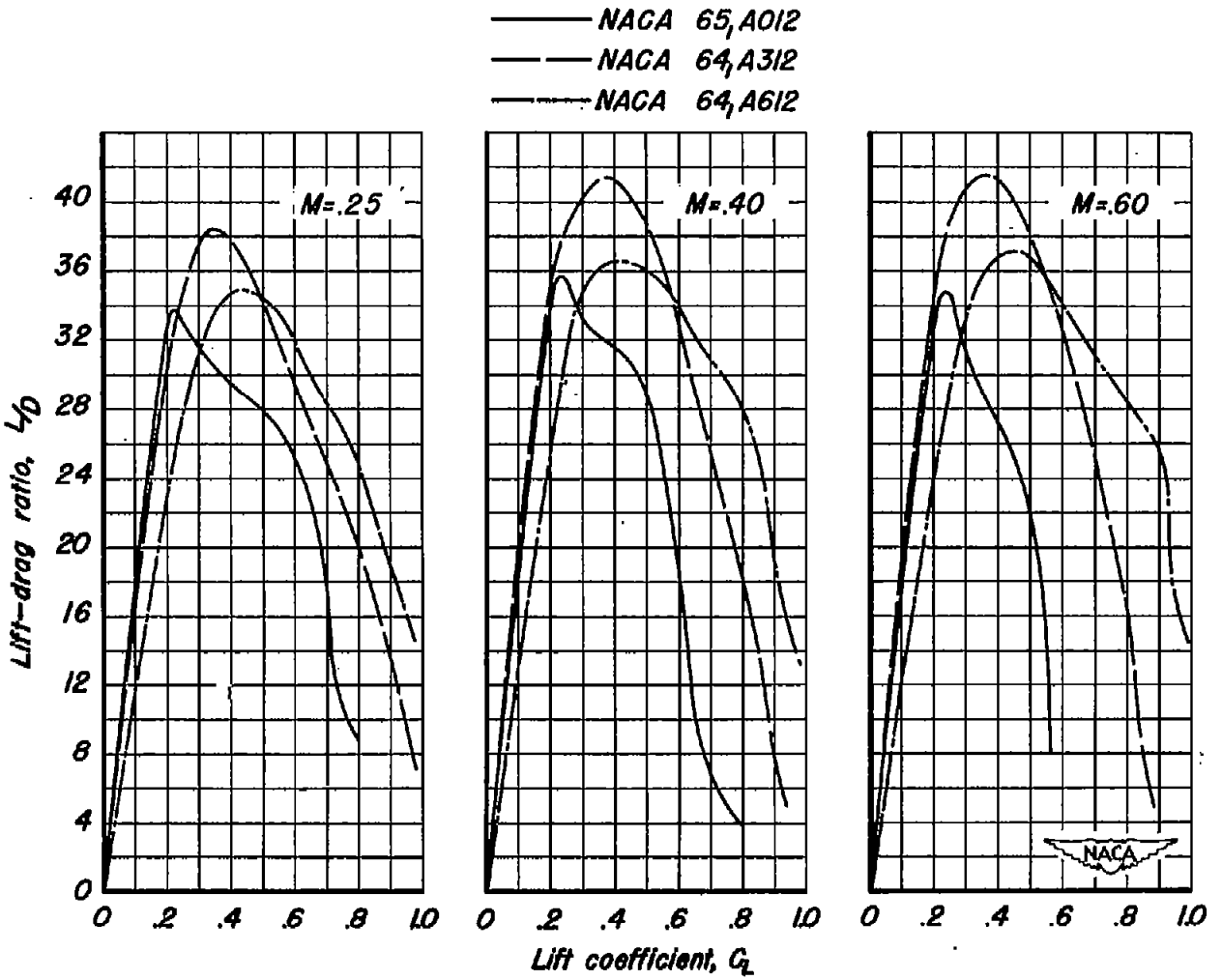

(a) M, 0.25 to 0.60.

Figure 19.- The variation of lift-drag ratio with lift coefficient. A, 10; R, 2,000,000.

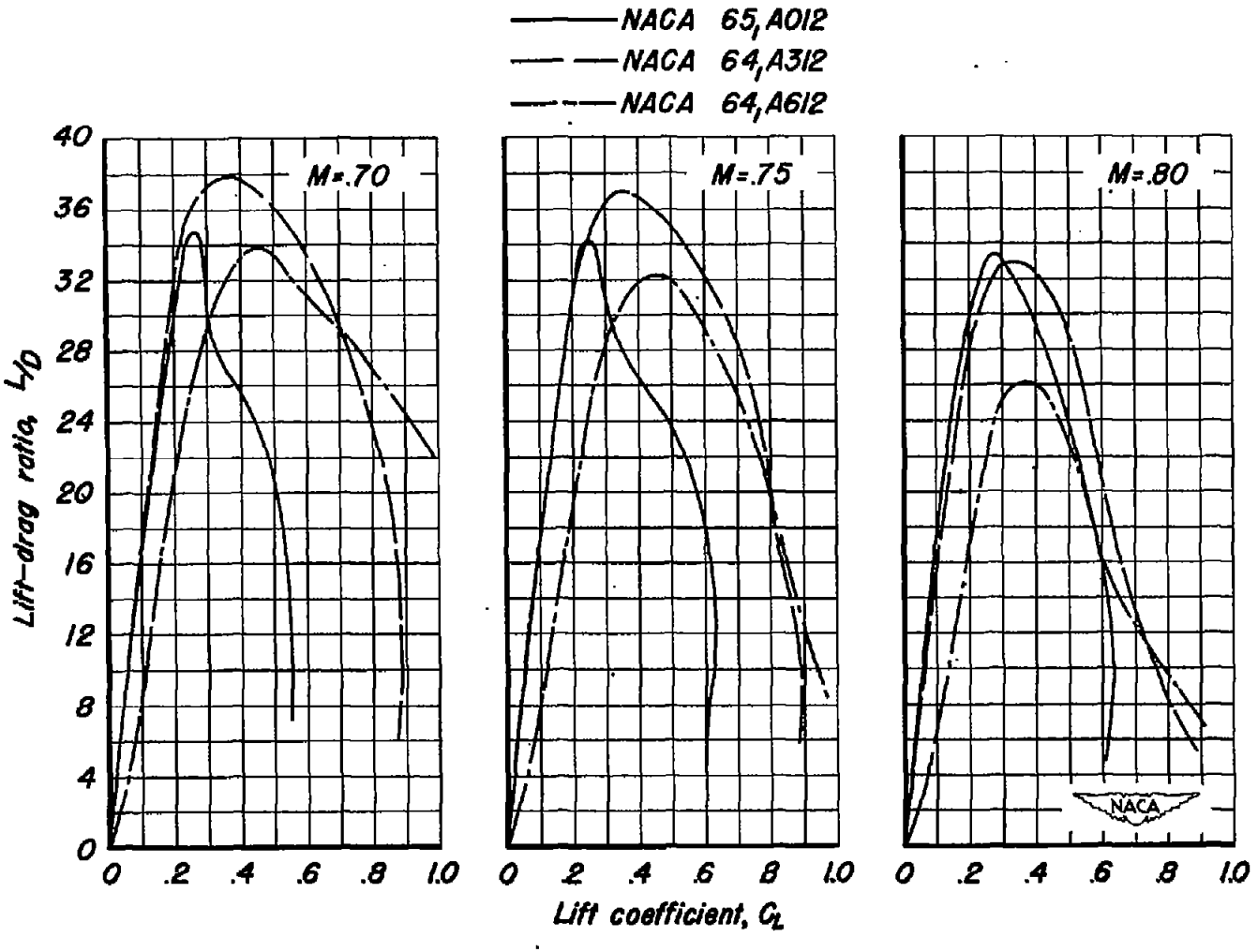

(b) M, 0.70 to 0.80.

Figure 19.- Continued.

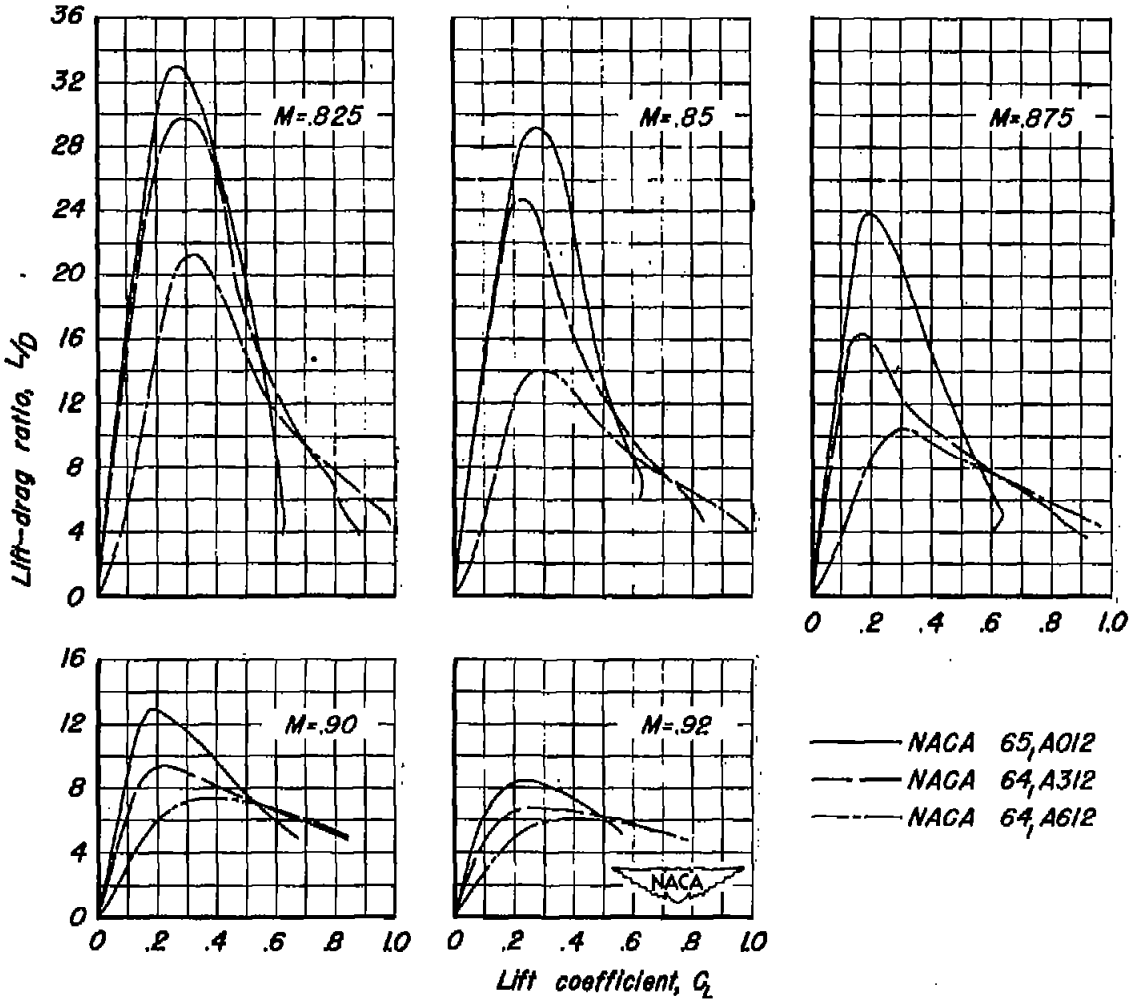

(c) M, 0.825 to 0.92.

Figure 19— Concluded.

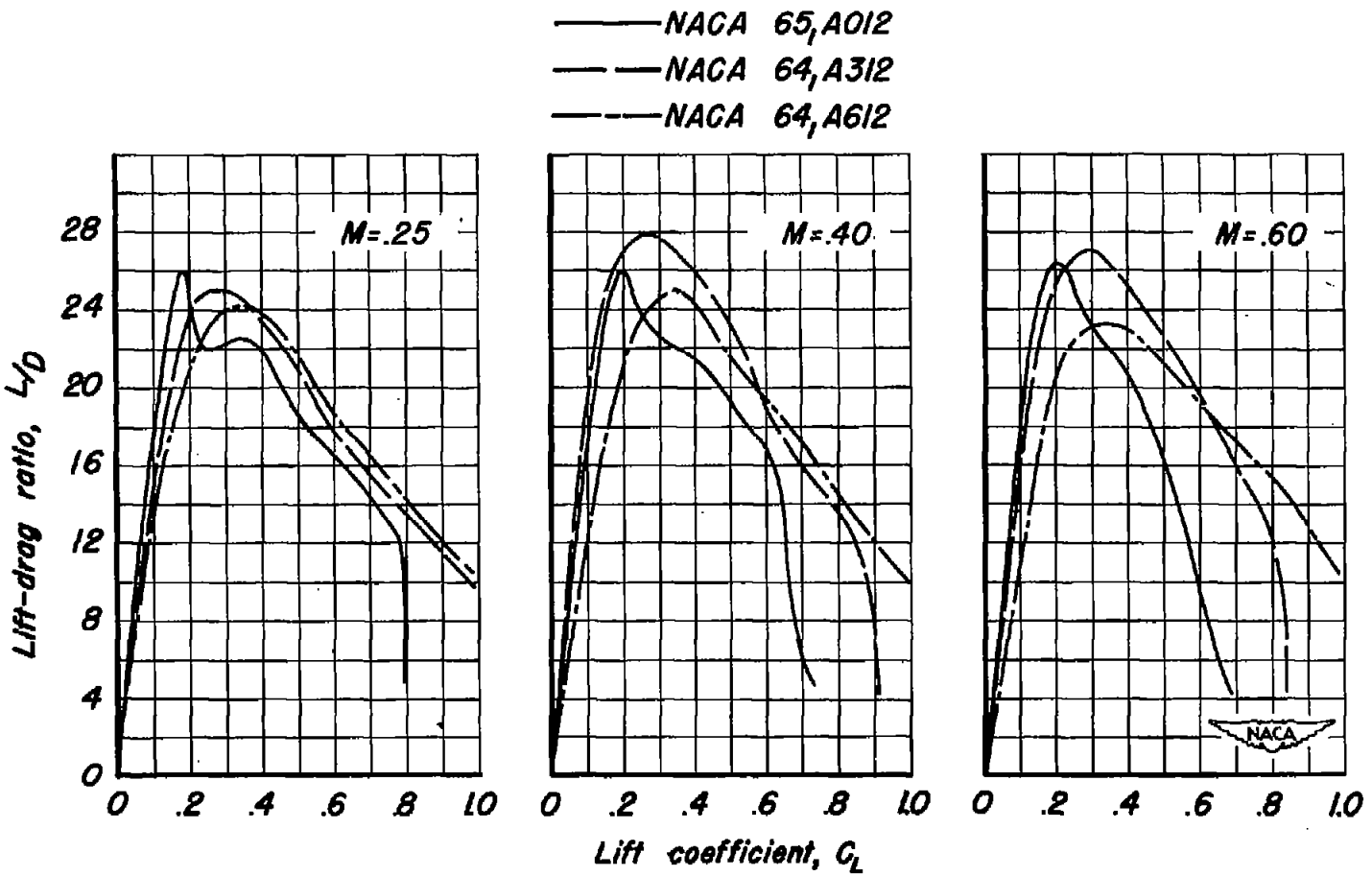

(a) M, 0.25 to 0.60.

Figure 20.- The variation of lift-drag ratio with lift coefficient. A, 5; R, 2,000,000.

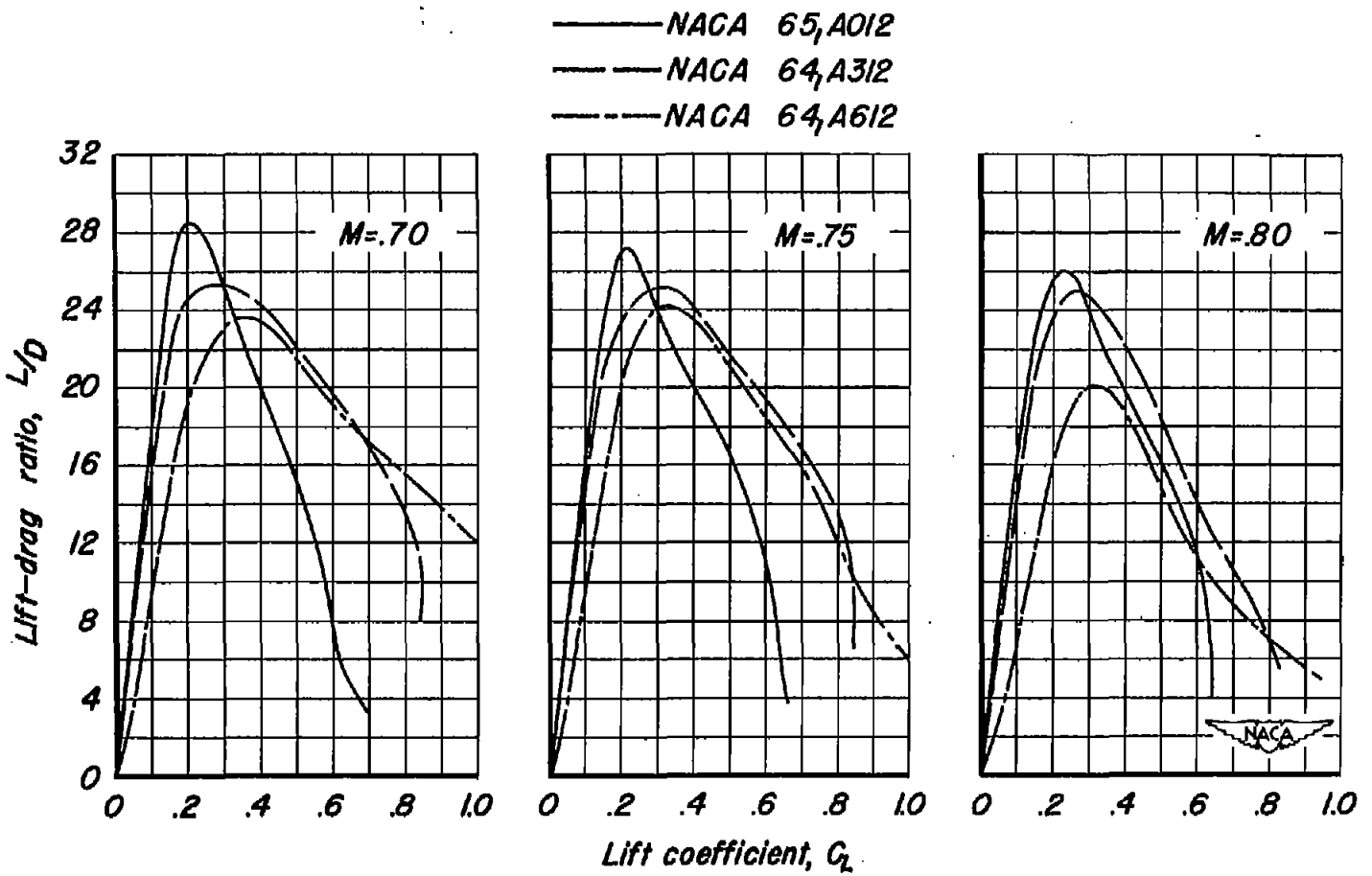

(b) M, 0.70 to 0.80.

Figure 20.– Continued.

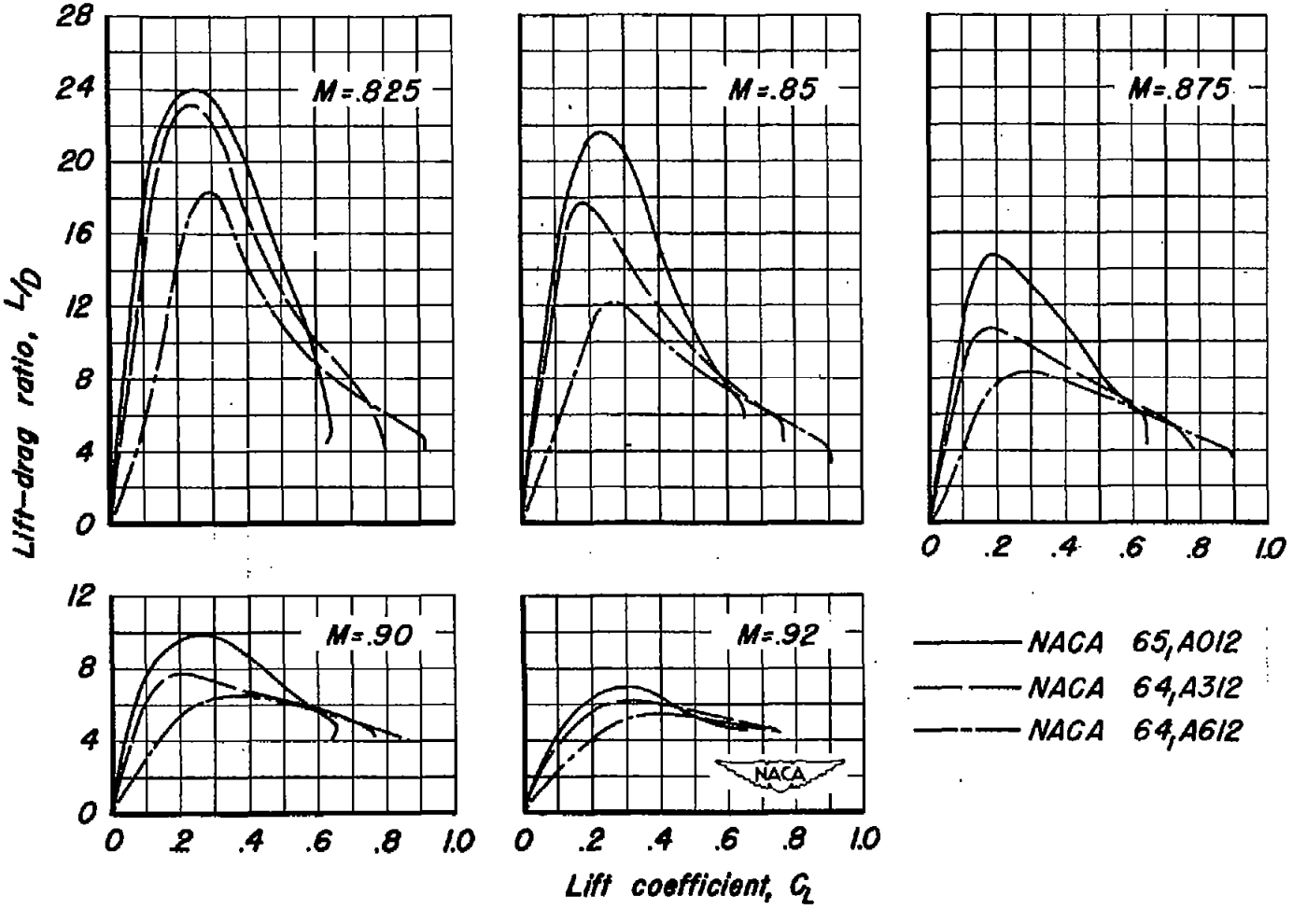

(c) M, 0.825 to 0.92.

Figure 20.— Concluded.